From Preferences to Prejudice: The Role of Alignment Tuning in Shaping Social Bias in Video Diffusion Models

Anonymous authors
Paper under double-blind review

Abstract

Recent advances in video diffusion models have significantly enhanced text-to-video generation, particularly through *alignment tuning* using reward models trained on human preferences. While these methods improve visual quality, they can unintentionally encode and amplify *social biases*. To systematically trace how such biases evolve throughout the alignment pipeline, we introduce VideoBiasEval, a comprehensive diagnostic framework for evaluating social representation in video generation. Grounded in established social bias taxonomies, VideoBiasEval employs an *event-based prompting* strategy to disentangle semantic content (actions and contexts) from actor attributes (gender and ethnicity). It further introduces multi-granular metrics to evaluate (1) overall ethnicity bias, (2) gender bias conditioned on ethnicity, (3) distributional shifts in social attributes across model variants, and (4) the temporal persistence of bias within videos. Using this framework, we conduct the first end-to-end analysis connecting biases in *human preference datasets*, their amplification in *reward models*, and their propagation through *alignment-tuned video diffusion models*. Our results reveal that alignment tuning not only strengthens representational biases but also makes them temporally stable, producing smoother yet more stereotyped portrayals. These findings highlight the need for bias-aware evaluation and mitigation throughout the alignment process to ensure fair and socially responsible video generation.

1 Introduction

Recent advancements in video diffusion models have remarkably improved the generation of high-quality videos from natural language prompts (Chen et al., 2024a; Wang et al., 2023a; Yuan et al., 2024; Li et al., 2024), unlocking potential across educational creation and professional simulations (Cho et al., 2024; Miller et al., 2024). To further enhance generation quality and controllability, a growing trend in state-of-the-art open-source models involves *alignment tuning* techniques, prominently through learning from human preferences (Wu et al., 2023; Xu et al., 2024; Li et al., 2024; Yuan et al., 2024; Liu et al., 2024a; Prabhudesai et al., 2024; Black et al., 2023; Ma et al., 2025). These approaches often employ reward functions trained on human preferences datasets (Wu et al., 2023; Kirstain et al., 2023a; Xu et al., 2024), utilizing frame-level comparisons to guide fine-tuning. While alignment tuning demonstrably improves the fluency and visual fidelity of generated videos, its inherent reliance on subjective notions of "preference" introduces a critical yet often overlooked challenge. These seemingly neutral judgments, potentially insensitive to diverse cultural and social contexts, can inadvertently solidify and propagate biased representations of identity groups within the generated video content (Qiu et al., 2023). In this work, we investigate a significant and underexplored factor influencing social representation in video diffusion models: **the crucial role of alignment tuning in shaping social bias in video diffusion models**.

Exploring this research requires a holistic evaluation framework—one that incorporates a probing method to elicit social attributes from video diffusion models, metrics to quantify the distribution of social biases within these models, and an analysis protocol capable of tracking changes in social attribute distributions

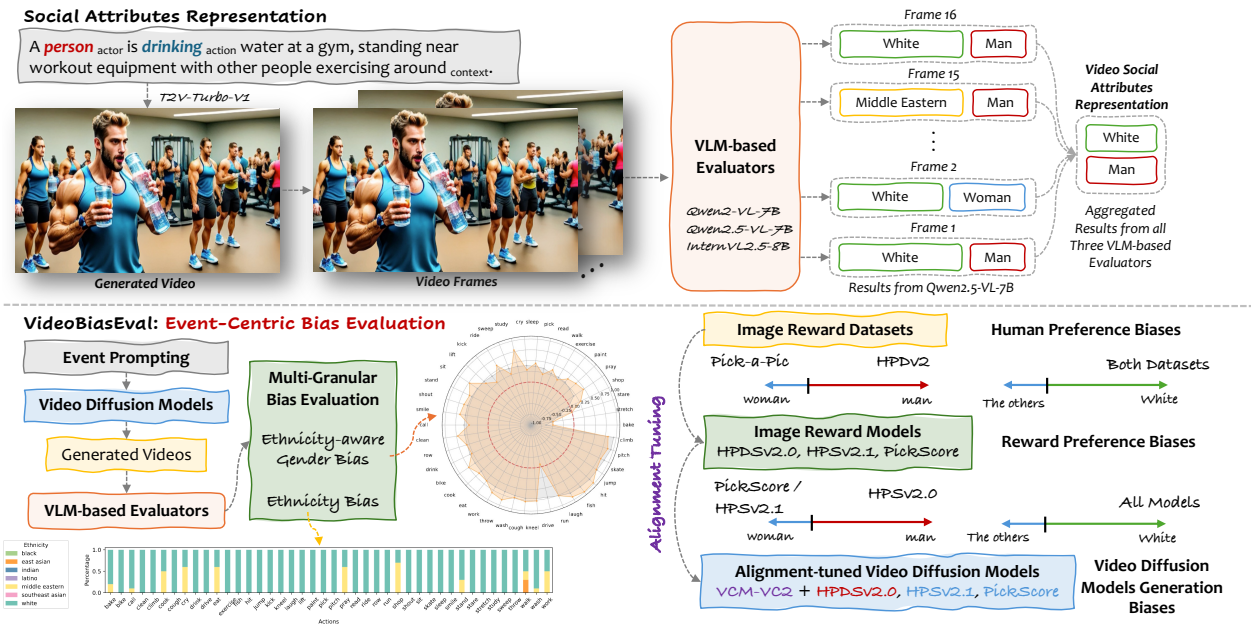

Figure 1: Overview of our work: (1) We introduce VIDEOBIASEVAL, a bias evaluation framework for video generation that leverages event-based prompts and multi-granular metrics to assess ethnicity and gender bias (bottom left, §3). The framework represents videos through social attribute annotations (top), where visual-language models (VLMs) infer actor attributes such as gender and ethnicity across frames and aggregate them for bias quantification §3.3). (2) We conduct the first comprehensive analysis of how image-based reward models, shaped by human-labeled preferences, influence the distribution of social attributes in diffusion-generated videos, disentangling human preference biases, reward preference biases, and their downstream impact on video diffusion model generation biases (bottom right, §5.1, §5.2, and §6).

before and after alignment. However, existing evaluation frameworks (Huang et al., 2024; Liu et al., 2024b; Sun et al., 2024) fall short in detecting and analyzing social biases due to three key limitations: (1) their reliance on prompts that do not adequately represent diverse social identities, thus limiting the analysis of how models portray or misrepresent these attributes; (2) the lack of comprehensive identity coverage and specific metrics, which hinders the ability of prior work to track the impact of alignment techniques on the distribution of social attributes; and (3) the absence of a dedicated method to track shifts in social attribute distributions before and after the application of alignment techniques.

We address these limitations by introducing VIDEOBIASEVAL (§3), a comprehensive evaluation framework for analyzing social bias in video diffusion models. The framework leverages *event*-based prompting and builds on established social bias taxonomies (Zhao et al., 2017; Hendricks & Nematzadeh, 2021; Cho et al., 2023; Qiu et al., 2023), allowing for precise control over both action types and actor identity attributes. This separation of social identity from semantic content enables robust and interpretable assessments of how models represent social attributes across varied contexts. Building on prior work in alignment and fairness within generative systems (Luccioni et al., 2023; Shen et al., 2023), we specifically focus on *gender* and *ethnicity*, two social dimensions with comparatively well-defined evaluative boundaries. Furthermore, the framework introduces multi-granular metrics that designed to assess (1) ethnicity bias, (2) gender bias conditioned on ethnicity, (3) shifts in social attribute distributions across different models, and (4) the temporal persistence of bias within videos. Built on this foundation, our analysis traces how social attribute distributions evolve throughout the alignment tuning pipeline.

We begin with an examination of demographic preferences embedded in human preference datasets, specifically HPDv2 (Wu et al., 2023) and Pick-a-Pic (Kirstain et al., 2023a) (§5.1). Next, we investigate how these patterns are inherited by image reward models, including HPSv2.0, HPSv2.1 (Wu et al., 2023), and PickScore

(Kirstain et al., 2023a) (§5.2). Finally, we fine-tune a video consistency model distilled from VideoCrafter-2 (Chen et al., 2023) using different image reward models (§6), enabling a detailed comparison of video outputs before and after alignment. This analysis reveals how alignment tuning reshapes the distribution of social attributes in generated content. Experimental results show that both human preference datasets exhibit non-neutral gender preferences and a strong imbalance favoring White representations. Reward models trained on these datasets inherit and amplify these social biases, which are then propagated through alignment-tuned video diffusion models. Alignment with male- or female-preferred reward models systematically shifts gender portrayals, while ethnic representation remains uneven across groups. Moreover, our Temporal Attribute Stability (TAS) analysis indicates that alignment tuning improves the consistency of social attribute portrayals over time but can also make biased representations more persistent and visually stable. These findings demonstrate that alignment tuning simultaneously enhances video quality and coherence while reinforcing or stabilizing existing social biases. They highlight the need for bias-aware evaluation and alignment strategies throughout the generative pipeline to ensure equitable and socially responsible video generation.

Furthermore, we examine whether controllable image reward datasets can be intentionally constructed by manipulating the distribution of social attributes (§7). We then assess whether training reward models on such curated datasets enables video diffusion models to generate outputs with controllable bias representations, thereby offering a potential path toward more equitable generative systems. Finally, we provide a comprehensive analysis of the changes in reward model preferences across 42 events and the resulting shifts in video model bias before and after alignment tuning. Building on these findings, we further offer guidance for addressing observed biases, outlining how targeted data composition and counter-biased reward modeling can serve as effective strategies for mitigating representational disparities in future generative video systems.

We make three key contributions: (1) We introduce VideoBiasEval, a comprehensive framework for evaluating social bias in video generation, which leverages event-based prompting and multi-granular metrics to assess ethnicity bias, gender bias conditioned on ethnicity, and temporal stability of social attributes across videos. (2) We present the first end-to-end analysis connecting *human preference datasets*, *reward models*, and *alignment-tuned video diffusion models*, revealing how social biases are inherited, amplified, and stabilized throughout the alignment pipeline. (3) Through systematic experiments, we demonstrate that preference alignment not only improves perceptual quality and temporal coherence but also reshapes—and in some cases reinforces—the social composition of generated content. Building on these findings, we offer guidance for addressing observed biases through controllable preference modeling, showing how targeted data composition and counter-biased reward design can effectively steer video diffusion models toward more equitable generative behavior.

2 Related Work

T2V Evaluation. Recent evaluation benchmarks such as VBench Huang et al. (2024), EvalCrafter Liu et al. (2024b), and T2V-CompBenchSun et al. (2024) evaluate text-to-video models using metrics like Fréchet Video Distance Unterthiner et al. (2019), CLIP-Score Hessel et al. (2021), and object consistency, yet they overlook who is depicted and how identities are portrayed. GRiT-based metrics Wu et al. (2025) may verify that a "doctor" appears, but fail to flag when all doctors are white men. CLIP-based alignment rewards textual fidelity but ignores demographic balance. To ensure fair and trustworthy evaluation, T2V benchmarks must move beyond surface-level metrics and explicitly audit the distribution of social attributes across outputs. Our work meets this need by introducing an event-centric framework that quantifies gender and ethnicity-aware biases throughout the entire T2V generation pipeline.

Bias Evaluation in Generative Models. Most existing studies on social bias in text-to-image or language generation focus on static, single-frame outputs such as portraits or isolated object scenes. Approaches like StableBias Luccioni et al. (2023), DALL-Eval Cho et al. (2023), and SocialCounterfactuals Howard et al. (2024) primarily tally identity frequencies but seldom examine what those identities are portrayed *doing*. Even recent benchmarks that track demographic representation often evaluate each image independently, which conceals recurring patterns such as the tendency to depict men in authoritative roles and women in supportive ones. By neglecting to analyze actors, actions, and context jointly, these evaluations fail to capture role-specific stereotypes and cannot reveal bias in narrative or temporal settings. We address this limitation

by auditing at the event level, disentangling actor attributes from actions and environments to uncover how social representation shifts across different scenarios.

3 VideoBiasEval

We introduce VideoBiasEval, a comprehensive framework for evaluating social biases in video generation models. Our approach leverages event-based prompting, where we systematically vary the gender and ethnicity of characters across a diverse set of real-world events (§3.1). Using these structured prompts, we generate videos with state-of-the-art diffusion models (§3.2). To quantify consistency and fairness in identity portrayals, we extract social attribute representations from the generated videos and perform a multi-granular evaluation across event categories (§3.3). Figure 2 illustrates representative prompts and demonstrates how social attributes are captured and analyzed from the generated outputs.

Prompt Template	A/An [actor] is baking a batch of cookies in a cozy kitchen, with warm light and the aroma of vanilla filling the air.			
Actors	Person	Person	Indian Person	Southeast Asian Person
Models	Video-Crafter-V2	T2V-Turbo-V1	T2V-Turbo-V1	T2V-Turbo-V1
Random Four Frames of Generated Videos				
Social Attributes Representations	(Man, White)	(Man, White)	(Man, Indian)	(Woman, Southeast Asian)

Figure 2: Illustration of videos generated by different diffusion models using varied prompt templates that specify actor attributes as detailed in §3.2. The main character's social attributes, including gender and ethnicity, are extracted using our proposed VLM-based evaluation method described in §3.3.

3.1 Event Definition

We investigate whether video generation models exhibit social biases in their portrayals of *events*, focusing on how different actors are visually represented while performing actions. Such biases often appear as imbalanced portrayals across *gender* or *ethnic* groups, reinforcing stereotypes and undermining fairness—patterns documented in prior work (Bolukbasi et al., 2016; Sun & Peng, 2021; Zajko, 2021). To systematically examine these effects, we represent each event as a tuple $\langle p, a, c \rangle$, where an actor p performs an action a within a context c. Our analysis centers on *socially associated actions*—those historically tied to identity-related stereotypes—following prior studies (Zhao et al., 2017; Garg et al., 2018; Cho et al., 2023; Qiu et al., 2023). This formulation enables us to assess how demographic attributes influence visual depictions across generated videos and to quantify systematic biases in model behavior.

Controlled Attribute Space. Our attribute design intentionally balances coverage and control. We analyze four gender categories and seven ethnic groups combined with 42 actions—choices grounded in established social bias taxonomies and prior benchmark conventions. This deliberately bounded setup enables the first *end-to-end tracing of bias propagation* in video generation, allowing clear attribution and interpretability while maintaining reproducibility. Expanding to open-ended or intersectional attributes is a promising next step; however, a well-defined and theoretically anchored scope is crucial for isolating representational disparities before scaling to unconstrained scenarios.

Actors. Each actor (p) is depicted with gender and ethnicity attributes to facilitate structured analysis of social bias. For gender, we adopt the *four* categories proposed by Luccioni et al. (2023): man, woman, the neutral term "person," and non-binary person. Although inclusive, this schema cannot capture the full diversity of gender identities but offers clear evaluative boundaries for controlled analysis. For ethnicity, we employ *seven* groups—White, Black, Indian, East Asian, Southeast Asian, Middle Eastern, and Latino—following

Karkkainen & Joo (2021) and U.S. Census Bureau conventions. While these categories aim to be inclusive, they are socially constructed and not intended to be exhaustive or universally representative.

Actions. We examine 42 actions (a)—*bake, bike, call, clean, climb, cook, cough, cry, drink, drive, eat, exercise, fish, hit, jump, kick, kneel, laugh, lift, paint, pick, pitch, pray, read, ride, row, run, shop, shout, sit, skate, sleep, smile, stand, stare, stretch, study, sweep, throw, walk, wash, work*—previously identified in the literature as statistically associated with particular genders or ethnic groups (Zhao et al., 2017; Garg et al., 2018; Cho et al., 2023; Qiu et al., 2023). These actions were selected not only for their well-documented social associations but also for their high visual distinctiveness and ease of depiction in short video clips, which ensures reliable annotation and interpretability of model outputs. This carefully curated yet socially meaningful action set establishes a reproducible foundation for future extensions toward more complex, culturally specific, or temporally dynamic event scenarios.

3.2 Event Prompting Template

To generate diverse yet systematically comparable prompts, we adopt the template: "A/An `[actor]` is `[action]`-ing `[context]`." Here, `[action]` spans the 42 curated activities, while `[context]` introduces situational variety without altering the semantic identity of the action. To disentangle the influence of demographic attributes, we define two prompting conditions: (1) `Person-only`, which uses "person" as the `[actor]`, and (2) `Ethnicity+Person`, which appends an ethnic descriptor to "person." Table 1 summarizes the prompt distribution and presents illustrative examples. Because the `ethnicity+person` condition inherently encodes ethnic information, an additional `ethnicity-only` setting is unnecessary for isolating ethnicity effects. Overall, this controlled event-prompting framework ensures that observed disparities can be reliably attributed to demographic conditioning rather than uncontrolled contextual drift—an essential property for reproducible bias auditing in generative video models.

Settings	# of Prompts	Examples
Person Only	168	A person is **baking** cookies in a cozy kitchen, with warm light and the aroma of vanilla filling the air.
Ethnicity + Person	1176	An *East Asian* person is **baking** cookies in a cozy kitchen, with warm light and the aroma of vanilla filling the air.

Table 1: Statistics of Social Bias Evaluation Prompts for Video Generation. Each prompt explicitly highlights the actor's *ethnicity* (when specified), the **action**, and the surrounding context, providing a structured basis for analyzing social representations in generated videos.

3.3 Multi-Granular Event-Centric Bias Evaluation

We propose a multi-granular evaluation protocol that captures both *fine-grained frame dynamics* and *aggregated video-level fairness*, enabling consistent assessment of how demographic portrayals emerge and persist over time. This design allows us to systematically analyze social biases in diffusion-generated videos across different temporal and representational granularities, revealing not only who is represented but also how consistently identities are maintained throughout the video.

Social Attribute Representations. We use *three* open-source vision–language models (VLMs)—Qwen2-VL-7B (Wang et al., 2024a), Qwen2.5-VL-7B (Yang et al., 2024), and InternVL2.5-8B (Chen et al., 2024b)—as automated judges to perform frame-wise classification of social attributes. For each generated video, we uniformly sample 16 frames and prompt the VLMs to independently infer the depicted *gender* and *ethnicity* in each frame. Each model outputs a gender label $g \in G = \{\text{man, woman}\}$ and an ethnicity label $e \in E = \{\text{White, Black, Indian, East Asian, Southeast Asian, Middle Eastern, Latino}\}$. Frame-level predictions are first aggregated within each model via majority voting to obtain video-level labels, and then fused across models through an ensemble strategy. This multi-model "VLMs-as-judges" ensemble enhances robustness and mitigates idiosyncratic biases or misclassifications from individual models (Qiu et al., 2024b). Representative classification prompts and example video outputs are shown in Figure 2. The resulting *frame-* and *video*-level social-attribute representations enable systematic evaluation of how well each generated video aligns with the intended demographic attributes specified in its prompt. The upper portion of Figure 1 illustrates this pipeline for deriving structured social-attribute representations. To ensure reliability and fairness, we further conduct human–model correlation analyses detailed in §4.

Temporal Attribute Stability. To complement static frame-level evaluation, we introduce a new temporal metric that directly quantifies the *intra-video stability* of social attribute representations over time. For each video, the **Temporal Attribute Stability (TAS)** score is defined as the percentage of frames whose classified attributes match the final majority-voted label for the video. A high TAS indicates temporally coherent and stable demographic portrayal, while a low TAS reflects attribute "flickering" or inconsistent identity depiction across frames—a critical temporal artifact in biased or unstable generation processes.

Beyond frame and temporal consistency, we further assess whether models generate socially balanced representations when aggregating across videos. The following video-level metrics quantify gender and ethnicity fairness across events and demographic groups.

Ethnicity-Aware Gender Bias. To assess how video generation models portray gender across different ethnic groups, we employ the **Proportion Bias Score for Gender** (PBS_G)[1]. For each action and ethnicity group, PBS_G is defined as $\text{PBS}_G = (N_{\text{man}} - N_{\text{woman}})/N_{\text{total}} \in [-1, 1]$, where where N_{man} and N_{woman} denote the number of representations depicting men and women, respectively, and N_{total} is their sum. A *positive* PBS_G indicates a bias toward *male* representations, a *negative* value indicates a bias toward *female* representations, and values *near zero* suggest *balanced* gender representation. By computing PBS_G under the `ethnicity+gender` condition, we capture how gender portrayals vary within each ethnic group—revealing whether models exhibit consistent gender balance across demographics or amplify gender disparities unevenly across ethnicities. An *ideal* model would achieve $\text{PBS}_G \approx 0$ for all ethnic groups, indicating equitable gender representation independent of ethnicity.

Ethnicity Bias. To evaluate how video generation models represent different ethnic groups, we employ two complementary metrics: the **Representation Deviation Score for ethnicity** (RDSe) (Feldman et al., 2015; Mehrabi et al., 2021) and **Simpson's Diversity Index** (SDI) (Simpson, 1949). For each ethnicity group $e \in E$, we define its representation proportion as $P_e = N_e/N_{\text{total}}$, where N_e denotes the number of outputs identified as ethnicity e, and N_{total} is the total number of outputs with identifiable ethnicity. The first metric, $\text{RDS}_e = P_e - 1/|E|$, quantifies how much each group's representation deviates from an ideal uniform distribution, where $1/|E|$ reflects perfectly balanced coverage across all groups. A *positive* RDS_e indicates *overrepresentation*, while a *negative* value signals *underrepresentation*. This metric thus reveals which ethnic groups are disproportionately favored or marginalized in model outputs, offering fine-grained, group-level insight into systemic disparities. Complementing this, the overall diversity of representations is measured by Simpson's Diversity Index, $\text{SDI} = 1 - \sum_{e \in E} {P_e}^2$, which captures the probability that two randomly selected outputs belong to different ethnicity groups. Higher SDI values indicate more diverse and balanced distributions, while lower values suggest concentration around a few dominant groups. Together, RDS_e and SDI provide a comprehensive perspective: RDS_e highlights *who is over- or underrepresented*, whereas SDI reflects *how balanced the overall representation landscape is*. These metrics jointly reveal whether generative models fairly portray global ethnic diversity or perpetuate skewed and homogeneous visual patterns. All metrics are computed under the `person-only` setting.

Bias Shift. Finally, we analyze *bias shift* between unaligned and aligned models to understand how alignment methods influence social fairness at the video level. For each metric, we compute ΔPBS_G, ΔRDS_e, and ΔSDI to quantify directional changes. Shifts toward more balanced gender ratios, reduced ethnic skew, or higher diversity indicate improvement. This complete evaluation suite—spanning frame dynamics, temporal stability, and video-level demographic fairness—provides a holistic understanding of bias formation and mitigation in diffusion-based video generation.

4 Social Biases in Video Generative Models

We apply our proposed evaluation framework to *four* state-of-the-art video diffusion models with varying alignment strategies. The **aligned** models include InstructVideo (Yuan et al., 2024), which is based on ModelScope (Wang et al., 2023a) and aligned with HPSv2.0, and T2V-Turbo-V1 (Li et al., 2024), which builds on VideoCrafter-2 (Chen et al., 2024a) and is aligned with HPSv2.1, InternVid2-S2 (Wang et al.,

[1]We exclude gender bias from this analysis because, in the absence of explicit ethnicity specifications, generative models predominantly produce representations of White individuals (Figure 12). Consequently, analyzing gender alone effectively reduces to examining gender bias within the White demographic (Figure 26).

Models	Average	White		Black		Latino		East Asian		Southeast Asian		India		Middle Eastern		Overall
	PBS_G	PBS_G	RDS	PBS_G	RDS	PBS_G	RDS	PBS_G	RDS	PBS_G	RDS	PBS_G	RDS	PBS_G	RDS	SDI
ModelScope (u)	0.4815	0.5683	**0.7690**	0.3912	-0.1952	0.6308	-0.1952	0.4406	-0.1810	0.4611	-	0.3938	-	0.4833	-0.1976	0.0538
InstructVideo (a)	0.5295	0.5584	**0.7833**	0.5114	-0.1976	0.6729	-0.1929	0.4282	-0.1976	0.5020	-	0.4878	-	0.5393	-0.1952	0.0267
Δ	+0.0480	-0.0099	+0.0143	+0.1202	-0.0024	+0.0421	+0.0023	-0.0124	-0.0166	+0.0409	-	+0.0940	-	+0.0560	+0.0024	-0.0271
Video-Crafter-V2 (u)	0.7581	0.7485	**0.6905**	0.6167	-0.1905	0.8599	-0.1952	0.6976	-0.1500	0.8272	-	0.8032	-	0.7560	-0.1548	**0.1252**
T2V-Turbo-V1 (a)	0.8306	0.8713	**0.6381**	0.8095	-	0.8599	-0.2476	0.7762	-0.2426	0.8929	-	0.7762	-	0.7664	-0.1476	0.1119
Δ	+0.0725	+0.1228	-0.0524	+0.1928	-	0.0000	-0.0524	+0.0786	-0.0926	+0.0657	-	-0.0270	-	+0.0104	+0.0072	-0.0133

Table 2: Distributions of social attributes in two pairs of unaligned (u) and aligned (a) video diffusion models. Each value represents the average score computed across 42 actions. A positive PBS_G score indicates a bias toward generating man characters (man-preference), while a negative score indicates a bias toward woman characters (woman-preference); values close to zero suggest balanced gender representation. We annotate man-preference with (+) and woman-preference with (−). For RDS_e, a positive score reflects the overrepresentation of a specific ethnicity, while a negative score reflects underrepresentation; these are marked with (+) and (−), respectively. Finally, a higher SDI score indicates greater balance and diversity in ethnic representation across the generated outputs.

2024b), and ViCLIP (Wang et al., 2023b). Their **unaligned** counterparts, ModelScope and VideoCrafter-2, serve as baselines for controlled comparisons.

To compute the social bias distribution, as outlined in §3, we generate videos with each prompt 10 times per model with different random seeds and average the results to reduce sampling variance. Table 2 reports two social bias metrics: ethnicity-aware gender bias (PBS_G) and ethnic representation distribution (RDS_e and SDI). Additional analysis across 42 actions appears in Appendix A.

Ethnicity-Aware Gender Bias. We evaluate gender portrayals under the `ethnicity+person` condition using the previously defined PBS_G metric. All models exhibit a consistent male bias, with average PBS_G values remaining above zero across all ethnic groups. Moreover, *alignment tuning amplifies this imbalance*: InstructVideo and T2V-Turbo-V1 show PBS_G increases of 0.04 and 0.0725, respectively, indicating that preference-based fine-tuning may worsen gender disparity rather than alleviate it. Figures 5 to 11 presents the PBS_G scores across 42 actions for each ethnicity group.

Ethnicity Bias. Under the `person-only` condition, we analyze models' representation balance using the previously defined RDS_e and SDI metrics. All models show a pronounced overrepresentation of White individuals, though the magnitude varies. ModelScope exhibits the strongest imbalance ($RDS_{White} = 0.769$, SDI = 0.0538), which is further amplified by alignment tuning in InstructVideo ($RDS_{White} = 0.783$, SDI = 0.0267). VideoCrafter-2 achieves moderately improved balance ($RDS_{White} = 0.6905$, SDI = 0.1252), while T2V-Turbo-V1 further reduces White dominance ($RDS_{White} = 0.6381$) but at the cost of lower diversity (SDI = 0.1119). Overall, while alignment tuning may alleviate certain ethnic skews, it can also suppress demographic diversity, suggesting a trade-off between bias reduction and representational variety. Figure 12 show the ethnicity bias across 42 actions.

Human Evaluation. To ensure the reliability of our VLM-based evaluators, we conduct human verification across 400 generated videos annotated by *three* independent annotators for gender and ethnicity. Our ensemble of three open-source VLMs—aggregated via majority voting—shows strong alignment with human judgments, achieving Pearson correlations of 0.89 (gender) and 0.73 (ethnicity). Agreement metrics further confirm high consistency: average Cohen's Kappa scores of 0.91 for gender and 0.78 for ethnicity, and inter-annotator agreement (Fleiss' Kappa) of 0.92 (gender) and 0.82 (ethnicity). These results, stable across both verification rounds, demonstrate that our VLM-based ensemble provides a robust, scalable, and human-aligned approach for large-scale social attribute evaluation.

These findings lead to our central research question: **How does alignment tuning shape the distribution of social attributes in video generative models?** To answer this, we (1) analyze demographic distributions embedded in the *image reward datasets* (§5.1), (2) examine the social biases in the trained *reward models* (§5.2), (3) assess how these biased reward models influence the representation of gender and ethnicity in video outputs when used for *alignment tuning* (§6).

5 Social Biases in Image Reward Datasets and Reward Models

Using image-based reward models has become the *de facto* and state-of-the-art approach for alignment tuning in video diffusion models (Wu et al., 2023; Xu et al., 2024; Li et al., 2024; Yuan et al., 2024; Liu et al., 2024a; Prabhudesai et al., 2024; Black et al., 2023; Ma et al., 2025). Because these reward models are trained on static images yet guide learning in temporally coherent video generation, their inherent social biases can propagate and even amplify across frames. Understanding such bias transfer from reward datasets to trained reward models is therefore crucial—not only to uncover demographic disparities embedded in human-labeled image preferences, but also to reveal how these biases shape the temporal evolution of social attributes in generated videos.

5.1 Preference in Image Reward Datasets

We analyze *two* widely used image reward datasets to investigate human preference biases: HPDv2 (Wu et al., 2023) and Pick-a-Pic (Kirstain et al., 2023b). For each dataset, we extract gender, ethnicity, and action attributes from image captions using GPT-4o-mini, and classify attributes from images using three VLMs (Qwen2-VL-7B, Qwen2.5-VL-7B, InternVL2.5-8B). We then aggregate the social attributes from both caption and image modalities, retaining only instances featuring one of our predefined actions. After processing, HPDv2 contains 28,783 validated (images, caption, preference) tuples covering 29 actions, and Pick-a-Pic contains 14,958 across 19 actions. Each tuple presents two images, with a human annotator selecting the one that best matches the caption. To assess potential human preference biases, we measure how often annotators *prefer* specific gender or ethnicity representations for given actions.

We directly analyze preference pairs where the preferred image depicts one gender (*e.g.*, a man) and the dispreferred image depicts the other (*e.g.*, a woman), thereby capturing explicit gender preference patterns within individual comparison pairs. Figure 13 shows the gender preference bias across 42 actions in the two datasets. After filtering to ensure valid man–woman pairs, 26 out of 42 actions in **HPDv2** met our criteria. Among these, 69.23% (18/26) showed a preference for men, revealing a consistent **man-preferred** tendency. In contrast, in **Pick-a-Pic**, 18 out of 42 actions qualified, and 61.11% (11/18) showed a preference for women, indicating a relatively **woman-preferred** trend. Furthermore, Table 9 presents the ethnicity preference distributions across the two image reward datasets. Notably, both datasets exhibit a strong preference for the **White** group, 43.34% in HPDv2 and 40.08% in Pick-a-Pic, followed by East Asian and Indian representations. Despite certain actions showing distinct preferences (*e.g.*, "bake" favoring Black individuals and "fish" favoring East Asians), the overall distributions reveal collected human preferences may implicitly favor Western-centric aesthetics and representation. These imbalances in human preferences might risk propagating representational bias during reward model training, thereby reinforcing existing social inequities in downstream video generation. Collectively, our findings underscore the urgent need for more inclusive and demographically representative preference datasets that capture global diversity.

5.2 Preference in Image Reward Models

Building on our analysis of gender and ethnicity biases in human preference datasets, we next examine how such biases propagate through *reward models* trained on these datasets.

Benchmark Construction. To systematically evaluate social biases in reward models, we construct a controlled benchmark based on text-to-image (T2I) generation, inspired by HPDv2 (Wu et al., 2023) and ImageRewardDB (Xu et al., 2024). Using the event prompting templates introduced in Section 3.2, we employ FLUX (Labs, 2023), a state-of-the-art T2I model, to generate diverse image sets varying systematically across gender, ethnicity, and action dimensions. The benchmark includes *two* generation settings:

Settings	# of Prompts	Examples
Ethnicity + Person	294	An *East Asian* person is **baking** cookies in a cozy kitchen, with warm light and the aroma of vanilla filling the air.
Ethnicity + Gender	1176	An *East Asian* woman is **baking** cookies in a cozy kitchen, with warm light and the aroma of vanilla filling the air.

Table 3: Statistics of Benchmark Construction Prompts for Image Reward Models. Each prompt explicitly highlights the actor's *ethnicity* (when specified), the **action**, and the surrounding context, providing a structured basis for analyzing social representations on image reward models.

Figure 3: Image examples of our constructed benchmark for evaluating preference in image reward models with generation prompts: "A/An `[ethnicity]` `[gender]` is baking `[context]`." We only show the images with `[gender]` $\in$ {man, woman}.

(1) `Ethnicity+Person`, where prompts specify only the actor's ethnicity, and (2) `Ethnicity+Gender`, where both gender and ethnicity are explicitly indicated. Table 3 summarizes prompt coverage and provides representative examples. To ensure statistical robustness, we generate 100 images per prompt, resulting in a large and diverse evaluation set. Sample outputs are illustrated in Figure 3.

The use of FLUX is not meant to assume a bias-free generator, but rather to provide a **controlled and reproducible setting** to probe preference patterns in reward models. By conditioning on systematically varied demographic attributes, our benchmark isolates the effects of reward model preferences independent of generator artifacts. To ensure benchmark integrity, we conduct a human verification study. Three annotators independently reviewed 100 randomly sampled images and unanimously confirmed that 77% accurately represented the intended social attributes. This validation demonstrates that the benchmark reliably captures the gender and ethnicity cues necessary for robust bias evaluation in reward models.

Preference Bias Evaluation. We evaluate *four* image reward models: (1) HPSv2.0 (Wu et al., 2023), trained on the HPDv2 dataset; (2) HPSv2.1 (Wu et al., 2023), trained on the unreleased HPDv2.1 dataset; (3) PickScore (Kirstain et al., 2023b), trained on the Pick-a-Pic dataset; and (4) CLIP (Radford et al., 2021), which serves as the base model for HPSv2.0, HPSv2.1, and PickScore prior to fine-tuning on their respective image reward datasets. Table 4 reports two complementary bias metrics, ethnicity-aware gender bias (PBS_G) and ethnic representation distribution (RDS_e and SDI). Appendix C includes more implementation details and comprehensive analysis across 42 actions.

Models	Average	White		Black		Latino		East Asian		Southeast Asian		India		Middle Eastern		Overall
	PBS_G	PBS_G	RDS	PBS_G	RDS	PBS_G	RDS	PBS_G	RDS	PBS_G	RDS	PBS_G	RDS	PBS_G	RDS	SDI
CLIP	-0.0726	0.0343	**0.0182**	-0.1198	0.0002	-0.0934	-0.0013	-0.1315	0.0141	-0.0865	0.0094	-0.0508	-0.0299	-0.0607	-0.0108	**0.8495**
HPSv2.0	0.6039	0.6090	-0.0423	0.7341	-0.0069	0.6512	0.0237	0.4752	-0.0031	0.5192	-0.0100	0.5922	0.0070	0.6464	**0.0315**	0.8492
Δ	+0.6765	+0.5747	-0.0605	+0.8539	-0.0071	+0.7446	+0.0250	+0.6067	-0.0172	+0.6057	-0.0194	+0.6430	+0.0369	+0.7071	+0.0423	-0.0003
HPSv2.1	-0.0984	-0.0833	-0.0189	0.0257	-0.0321	-0.0031	**0.0382**	-0.3044	0.0091	-0.2181	-0.0099	-0.0006	-0.0077	-0.1053	0.0214	0.8470
Δ	-0.0258	-0.1176	-0.0371	+0.1455	-0.0323	+0.0903	+0.0395	-0.1729	-0.0050	-0.1316	-0.0193	+0.0502	+0.0222	-0.0446	+0.0322	-0.0025
PickScore	-0.1157	0.0321	0.0069	-0.0777	0.0279	-0.3479	-0.0118	-0.2257	**0.0316**	-0.2163	0.0115	0.1531	-0.0391	-0.1277	-0.0271	0.8483
Δ	-0.0431	-0.0022	-0.0113	+0.0421	+0.0277	-0.2545	-0.0105	-0.0942	+0.0175	-0.1298	+0.0021	+0.2039	-0.0092	-0.0670	-0.0163	-0.0012

Table 4: Preference bias of different reward models. All values represent *average* scores across 42 actions.

Ethnicity-Aware Gender Bias. We construct preference evaluation prompts in the format "A/An `[ethnicity]` person is `[action]`-ing `[context]`", covering all combinations of ethnicity and action (evaluation: `ethnicity+person`). For each preference prompt, we generate images using generation prompts in the format "A/An `[ethnicity]` `[gender]` is `[action]`-ing `[context]`", where gender, ethnicity, and action are explicitly specified (generation: `ethnicity+gender`). The evaluation prompt omits gender to measure reward model's inherent preference, while the generation prompt explicitly specifies gender. The reward scores

assigned to these images by a reward model are standardized using their mean and standard deviation. We then compute the average standardized score across the 100 images for each generation prompt. To compute the final PBS_G, we fix the ethnicity and action, and subtract the average standardized score for women from that for men. Because of the adaptation, PBS_G score here can be greater than one. A positive PBS_G score indicates a preference for men, while a negative score reflects a preference for women. CLIP shows a slight woman-preference bias (–0.0726). Fine-tuning on HPDv2 shifts HPSv2.0 toward a *strong* man-preference (+0.6039), consistent across ethnic groups. In contrast, PickScore (–0.1157) and HPSv2.1 (–0.0984) show woman-preference biases, with the latter's training data undisclosed. These shifts align with each model's training data, revealing consistent gender preferences across ethnicities. Figures 15 to 21 presents the PBS_G scores across 42 actions for each ethnicity group.

Ethnicity Bias. We use preference evaluation prompts in the form "A person is `[action]`-ing `[context]`" (evaluation: `person-only`). For each preference prompt, we have generated images using more specific generation prompts of the form "A/An `[ethnicity]` person is `[action]`-ing `[context]`", where the ethnicity and action are explicitly specified (generation: `ethnicity+person`). The evaluation prompt omits ethnicity to measure reward model's inherent preference, while the generation prompt explicitly specifies ethnicity. The reward scores for these images provided by a reward model are standardized with mean and standard deviation. We then compute the average standardized score across the 100 images for each generation prompt. To calculate RDS_e and SDI, we fix the action and apply softmax function (Bridle, 1990; Bishop, 2006) to normalize the scores for each ethnicity, indicating ethnicity preference within each action context. A positive RDS_e indicates overrepresentation of an ethnicity, while a negative score indicates underrepresentation. A higher SDI score corresponds to more balanced and diverse outputs across all groups. The base model, CLIP, slightly favors White individuals (RDS = 0.0182) and achieves the highest SDI score (0.8495), indicating relatively balanced ethnic representation. After fine-tuning, HPSv2.0 shifts toward Middle Eastern (RDS = 0.0315), HPSv2.1 toward Latino (RDS = 0.0382), and PickScore toward East Asian individuals (RDS = 0.0352). All show reduced SDI, indicating decreased ethnic diversity post-alignment. Figures 22 to 25 show the ethnicity bias across 42 actions.

6 Social Biases in Preference Alignment

Building on our analysis of gender and ethnicity biases in image reward models, we examine how preference alignment tuning affects bias in video generation. We fine-tune a Video Consistency Model distilled from VideoCrafter-V2 (VCM-VC2) (Li et al., 2024) using *three* image-text reward models, HPSv2.0, HPSv2.1, and PickScore, and compare social bias distributions before and after tuning to assess how each reward model shapes identity representation. Following the T2V-Turbo-V1 training protocol (Li et al., 2024), we incorporate reward feedback into the state-of-the-art paradigm–Latent Consistency Distillation process (Luo et al., 2023) by using single step video generation. During student model distillation from a pretrained teacher text to video model, we directly optimize the decoded video frames to maximize reward scores from the image-text alignment models, guiding each frame toward representations more aligned with human preferences. Video model post-training and inference details can be found in Appendix G.

We evaluate aligned video diffusion models using our evaluation framework (§4). Table 5 reports two metrics: PBS_G for gender imbalance across ethnic groups, and RDS_e and SDI for ethnicity representation disparity and overall output diversity. Appendix D includes more analysis across 42 actions.

Models	**Average**	**White**		**Black**		**Latino**		**East Asian**		**Southeast Asian**		**India**		**Middle Eastern**		**Overall**
	PBS_G	PBS_G	RDS	PBS_G	RDS	PBS_G	RDS	PBS_G	RDS	PBS_G	RDS	PBS_G	RDS	PBS_G	RDS	SDI
VCM-VC2	0.8034	0.7925	**0.6405**	0.7758	-0.2381	0.8090	–	0.7115	-0.2333	0.7945	–	0.8634	–	0.8071	-0.1690	0.1433
+ HPSv2.0	0.9116	0.9667	0.3667	0.9214	–	0.9667	–	0.8500	–	0.9214	–	0.9000	–	0.8548	-0.3667	0.1257
Δ	+0.1082	+0.1742	-0.2738	+0.1456	–	+0.1577	–	+0.1385	–	+0.1269	–	+0.0366	–	+0.0477	-0.1977	-0.0176
+ HPSv2.1	0.2267	0.1321	**0.4286**	0.2381	–	0.3738	–	0.1571	–	0.3619	–	0.1452	–	0.1786	-0.4286	0.0976
Δ	-0.5767	-0.6604	-0.2119	-0.5377	–	-0.4352	–	-0.5544	–	-0.4326	–	-0.7182	–	-0.6285	-0.2596	-0.0457
+ PickScore	0.3714	0.3429	**0.6833**	0.3357	-0.1810	0.7190	-0.1929	0.1450	-0.1952	0.4548	–	0.2500	–	0.3515	-0.1143	0.1467
Δ	-0.4320	-0.4496	+0.0428	-0.4401	+0.0571	-0.0900	-0.1929	-0.5665	+0.0381	-0.3397	–	-0.6134	–	-0.4556	+0.0547	+0.0034

Table 5: Social biases of aligned models. All values represent *average* scores across 42 actions.

Ethnicity-Aware Gender Bias. We evaluate gender portrayals under the `ethnicity+person` condition using the previously defined PBS_G metric. A positive PBS_G score indicates a tendency to depict men more frequently, while a negative score suggests a preference for women. The base model, VCM-VC2, demonstrates a strong man bias across all ethnicities, which becomes more pronounced with alignment using HPSv2.0. In contrast, alignment with HPSv2.1 and PickScore significantly reduces PBS_G, indicating a shift toward more balanced or woman-preferred outputs. This change reflects the underlying woman bias present in the HPSv2.1 and PickScore reward models, which steer the model away from the man-dominant bias of the base model. Figures 26 to 33 presents the PBS_G scores across 42 actions for each ethnicity group.

Ethnicity Bias. Under the `ethnicity-only` condition, we analyze models' representation balance using the previously defined RDS_e and SDI metrics. Positive values indicate overrepresentation, and negative values indicate underrepresentation. Overall demographic balance is measured using SDI, where higher values reflect more equitable representation. The base model, VCM-VC2, strongly favors White individuals (RDS = 0.6405), while Black, East Asian, and Middle Eastern groups are underrepresented. Alignment with HPSv2.1 reduces some disparities by improving balance for White and Black groups, but significantly decreases Latino representation (RDS = –0.4352) and lowers SDI, indicating reduced diversity. In contrast, PickScore achieves the highest SDI and produces more balanced representation across most ethnic groups, resulting in the most demographically equitable outputs. Figure 34 shows the ethnicity bias across 42 actions.

Model	**Attribute**	**Mean TAS (%)**	**Median TAS (%)**	**Std TAS (%)**	**Perfect Stability (100 %)**
VCM-VC2	Ethnicity	89.04	100.00	16.73	56.7
VCM-VC2	Gender	97.63	100.00	8.29	88.5
+ HPSv2	Ethnicity	$93.05_{+4.01}$	100.00	$13.58_{-3.15}$	$70.5_{+13.8}$
+ HPSv2	Gender	$99.67_{+2.04}$	100.00	$3.10_{-5.19}$	$98.3_{+9.8}$
+ HPSv2.1	Ethnicity	$96.32_{+7.28}$	100.00	$10.19_{-6.54}$	$83.3_{+26.6}$
+ HPSv2.1	Gender	$98.95_{+1.32}$	100.00	$5.19_{-3.10}$	$94.4_{+5.9}$
+ PickScore	Ethnicity	$94.06_{+5.02}$	100.00	$13.02_{-3.71}$	$75.6_{+18.9}$
+ PickScore	Gender	$98.84_{+1.21}$	100.00	$5.53_{-2.76}$	$94.1_{+5.6}$

Table 6: Temporal Attribute Stability (TAS) across models and attributes. A high TAS score indicates the actor's identity representation is stable and consistent throughout the video. A low TAS score indicates the representation 'flickers" or changes, a key temporal artifact. Subscripts in red and blue indicate relative improvements and degradations compared to the base model VCM-VC2.

Temporal Attribute Stability. Table 6 summarizes the temporal consistency of identity portrayals across alignment-tuned models. Overall, alignment substantially improves the *technical coherence* of video generation. For ethnicity, the mean TAS increases from 89.04% in the VCM-VC2 baseline to 96.32% after HPSv2.1 alignment, and the proportion of videos achieving perfect stability rises by 26.6 points (from 56.7% to 83.3%). Similar gains appear for gender, with stability reaching near saturation at 98.95% and 94.4% perfect stability. The standard deviation of TAS also consistently decreases (*e.g.*, –6.54 for ethnicity), indicating *more uniform frame-level consistency across videos*. However, this improvement in stability comes with an important caveat. When alignment models inherit biased preferences, the resulting stability can entrench rather than mitigate bias. For instance, HPSv2.0 alignment not only amplifies the overall man-preference bias (PBS_G rising from 0.8034 to 0.9116) but also locks that bias in temporally—with gender stability reaching 99.67% and nearly all videos (98.3%) achieving perfect stability. In other words, the model becomes *better at being biased*: it produces smoother, more coherent, yet more stereotyped portrayals. This finding highlights a critical insight revealed uniquely by our temporal evaluation framework: alignment tuning, while improving the perceptual and temporal quality of generation, can inadvertently make social bias more persistent and deeply embedded in the generative process. VideoBiasEval thus not only detects whether a model is biased but also exposes how alignment can make such bias temporally resilient—transforming representational artifacts into stable, systematic distortions.

Summary and Implications. Taken together, these findings demonstrate that preference alignment can both mitigate and amplify existing social biases, depending on the characteristics of the guiding reward model. While HPSv2.0 reinforces the base model's male- and White-preferred tendencies, HPSv2.1 and PickScore—both exhibiting woman-preferred reward patterns—successfully counteract the original man-

dominant bias, steering the aligned model toward more balanced portrayals. However, neither alignment achieves complete demographic parity, as residual disparities across ethnic groups persist. These observations suggest that the direction and magnitude of social bias in aligned video diffusion models are largely inherited from the bias profile of their reward models.

7 Controllable Preference Modeling for Video Diffusion Models

Building on prior findings, we next examine whether such biases can be made *controllable*. Specifically, we investigate if adjusting the distribution of social attributes in image preference datasets can systematically steer reward models—and consequently video diffusion models—toward more equitable or intentionally calibrated portrayals (Sheng et al., 2020). To make this concrete, we take **gender** as a case study, examining how varying gender composition in preference data influences the directional bias and alignment dynamics of the resulting reward and video models.

7.1 Image Reward Dataset Construction

We construct two reward datasets: a man-preferred version and a woman-preferred version, using images from §5.1 to guide diffusion models toward gender-specific representations. Each dataset includes 2.94 million preference pairs from the `Ethnicity+Gender` set, where each pair depicts the same action and ethnicity but differs by gender (*e.g.*, M-1 vs. W-1 in Figure 3). Prompts follow the format "A/An `[ethnicity]` person is `[action]`-ing `[context]`." In the man-preferred dataset, male images are labeled 1 and female images 0; the opposite applies in the woman-preferred dataset. To enhance face-free diversity, we also include 537,660 additional image pairs from HPDv2. When applied to a base model with man-preference bias, the woman-preferred dataset helps correct this imbalance and promotes more equitable gender representation.

7.2 Image Reward Model Development & Alignment Tuning

Leveraging the man-preferred and woman-preferred image datasets, we fine-tune two reward models on top of a pre-trained CLIP vision encoder: the Man-Preferred Reward Model ($\mathrm{RM_M}$) and the Woman-Preferred Reward Model ($\mathrm{RM_W}$). Each is optimized to reflect gender-specific aesthetic and representational preferences encoded in its respective dataset. As shown in Table 7, $\mathrm{RM_M}$ consistently assigns higher PBS_G scores across all demographic groups, aligning with man-preferred portrayals, whereas $\mathrm{RM_W}$ exhibits the opposite tendency, systematically favoring woman-preferred content. This clear divergence demonstrates that reward tuning effectively captures and amplifies gendered preferences. Reward model training and inference details can be found in Appendix F.

Models	Average	White	Black	Latino	East Asian	Southeast Asian	India	Middle Eastern
CLIP	-0.0726	0.0343	-0.1198	-0.0934	-0.1315	-0.0865	-0.0508	-0.0607
$\mathrm{RM_M}$	$1.5280_{+1.60}$	$1.6300_{+1.60}$	$1.5752_{+1.70}$	$1.5524_{+1.65}$	$1.4323_{+1.56}$	$1.4525_{+1.54}$	$1.5619_{+1.61}$	$1.4914_{+1.55}$
$\mathrm{RM_W}$	$-0.7448_{-2.27}$	$-0.6318_{-2.26}$	$-0.7943_{-2.37}$	$-0.8279_{-2.38}$	$-0.6282_{-2.06}$	$-0.6429_{-2.10}$	$-0.8846_{-2.45}$	$-0.8042_{-2.30}$

Table 7: Preference bias of reward models. All values represent *average* scores across 42 actions.

We intentionally do not train a "fair" or demographically neutral reward model. As discussed in §6, the base video generator (*e.g.*, VCM-VC2) already exhibits a pronounced man bias. Under such asymmetric initialization, a neutral reward signal would merely reinforce existing imbalances rather than correct them. To counteract this skew, we employ a deliberately counter-biased reward model—specifically, the woman-preferred $\mathrm{RM_W}$, analogous to HPSv2.1—which actively steers generation toward gender equilibrium. This targeted alignment strategy yields markedly more balanced portrayals, demonstrating that directional reward tuning can serve as an effective corrective mechanism for bias mitigation.

Building upon these reward models, we further apply $\mathrm{RM_M}$ and $\mathrm{RM_W}$ to guide preference alignment of the base video diffusion model (VCM-VC2). Using the same preference-optimization framework, we obtain two aligned variants: one tuned toward man-preferred and the other toward woman-preferred content. As shown in Table 8, alignment with $\mathrm{RM_M}$ increases PBS_G scores across all demographic groups, reinforcing

man-preference bias, whereas alignment with RM_W substantially reduces these scores, indicating a strong shift toward woman-preference bias. These results confirm that our controllable preference modeling framework enables fine-grained modulation of gender bias in video generation, offering a principled and flexible means to amplify or mitigate social tendencies in diffusion-based models. Moreover, achieving the most balanced aligned video generator can be framed as a data composition problem: by systematically adjusting the proportion of man- and woman-preferred samples in the reward dataset, one can identify an optimal mixture that minimizes overall bias while preserving aesthetic fidelity. This insight highlights a promising direction for dataset-driven bias control in alignment tuning. Figures 35 to 39 presents the PBS_G scores across 42 actions for each ethnicity group.

Models	Average	White	Black	Latino	East Asian	Southeast Asian	India	Middle Eastern
VCM-VC2	0.8034	0.7925	0.7758	0.8690	0.7115	0.7945	0.8634	0.8071
+ RM_M	$0.9584_{+0.16}$	$0.9595_{+0.17}$	$0.9524_{+0.18}$	$0.9756_{+0.11}$	$0.9437_{+0.23}$	$0.9447_{+0.15}$	$0.9640_{+0.10}$	$0.9709_{+0.16}$
+ RM_W	$0.3082_{-0.50}$	$0.3341_{-0.46}$	$0.3913_{-0.38}$	$0.3314_{-0.54}$	$0.1008_{-0.61}$	$0.2639_{-0.53}$	$0.3446_{-0.52}$	$0.3894_{-0.42}$

Table 8: Social biases of aligned models. All values represent *average* scores across 42 actions.

Summary and Implications. Our controllable preference modeling framework demonstrates that bias in video diffusion models can be systematically directed through the construction and tuning of social-attribute-aware reward datasets. By varying gender composition in preference data, we show that reward models learn and transmit directional biases—reinforcing or counteracting existing tendencies in base generators. Importantly, introducing counter-biased reward models (*e.g.*, woman-preferred RM_W) can actively correct skewed portrayals, producing more balanced and socially representative generations. Beyond binary control, these results suggest a continuous axis of alignment, where nuanced mixtures of man- and woman-preferred data yield tunable trade-offs between bias mitigation and aesthetic coherence. The sensitivity analysis across 42 actions further reveals that even semantically neutral activities can exhibit large gender shifts under alignment, underscoring the need for fine-grained, event-level auditing. Overall, our findings highlight that dataset composition, rather than architectural intervention alone, offers a powerful and interpretable lever for steering the social behavior of generative models.

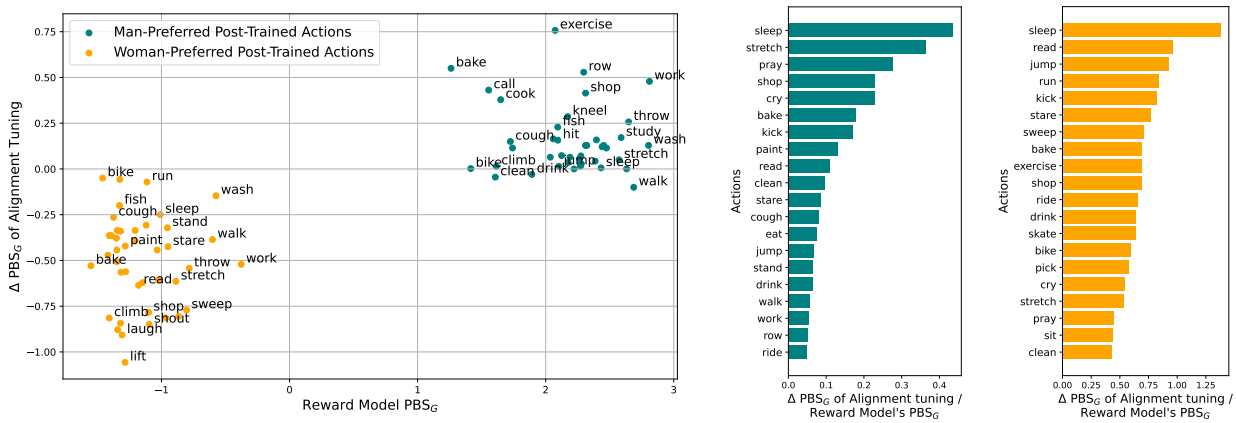

(a) Δ PBS_G of video generation model before and after alignment tuning by RM_M and RM_W. Results are broken down into actions. Figure 4b and Figure 4c are based on this figure.

(b) Sensitive actions in man-preferred alignment tuning.

(c) Sensitive actions in woman-preferred alignment tuning.

Figure 4: Action-level impact of alignment tuning guided by RM_M and RM_W.

Which Actions Are Most Sensitive During Alignment Tuning? We investigate how specific actions respond to gender-oriented reward model tuning by measuring changes in PBS_G scores before and after alignment. As shown in Figure 4a, actions cluster distinctly by the reward model that guides tuning: alignment with RM_M (teal) amplifies male-preferred portrayals in activities such as *exercise*, *row*, and *cook*, while alignment with RM_W (orange) shifts representations toward women-preferred actions like *bake*, *sleep*, and

sweep. Figure 4b and Figure 4c further quantify these shifts by ranking actions according to their normalized sensitivity (*i.e.*, $\Delta\text{PBS}_\text{G}$ divided by each reward model's baseline PBS_G). The top-ranked actions—*sleep*, *stretch*, and *read*—emerge as the most sensitive under both man- and woman-preferred tuning, revealing that even socially neutral or domestic activities can exhibit pronounced gender bias once alignment is applied. Together, these results highlight that alignment tuning induces systematic, action-specific bias amplification, and demonstrate the effectiveness of our event-centric evaluation framework in exposing fine-grained behavioral sensitivities across gendered dimensions.

8 Conclusion

In summary, our work exposes and investigates key blind spots in evaluating social bias within text-to-video generation. Through the introduction of VideoBiasEval, we establish a comprehensive framework that decouples identity attributes from content semantics and systematically tracks how alignment tuning reshapes social representations. Our analyses demonstrate that reward-model-based alignment not only inherits but frequently amplifies existing biases encoded in human preference data. These findings highlight the importance of integrating bias auditing and mitigation throughout every stage of the video generation pipeline, advancing the development of more equitable and socially aware generative systems.

Limitations

While our work presents a comprehensive evaluation of social biases introduced through alignment tuning in video diffusion models, several limitations warrant further consideration. *First*, our analysis focuses on two social dimensions, gender and ethnicity, using predefined categories based on U.S. Census conventions and prior literature. These categories, while practical for controlled evaluation, are inherently socially constructed and cannot fully capture the fluidity, intersectionality, or cultural nuances of identity Yin et al. (2024); Qiu et al. (2024a; 2025). Future work should explore richer identity representations, including intersectional groups. *Second*, our VLM-based evaluators, though validated against human judgments, rely on image-level classification and may exhibit their own biases or inaccuracies, particularly when interpreting identity in stylized or ambiguous frames. While we ensemble multiple models to mitigate this, ground truth annotations for a larger and more diverse set of videos would further strengthen the reliability of our measurements. *Third*, we primarily assess alignment impacts under a specific training strategy (single-step latent consistency distillation) and a limited set of reward models. Other training protocols, such as RL-based tuning or multi-turn video instruction alignment, may exhibit different bias dynamics not captured in our study. *Fourth*, our controllable preference modeling experiments, while demonstrating the feasibility of targeted bias modulation, are constrained to synthetic manipulations of gender preference. These interventions do not address broader questions of value alignment, normative appropriateness, or long-term societal impact, which are crucial for the responsible deployment of generative video systems. *Lastly*, our evaluation framework, VideoBiasEval, is currently benchmarked on a fixed set of 42 socially associated actions. While this enables fine-grained control, it may limit generalizability to open-ended generation settings or novel actions not covered in our taxonomy. We hope that these limitations encourage further research into holistic, culturally grounded, and ethically aligned evaluation pipelines for video generative models.

References

Christopher M. Bishop. *Pattern Recognition and Machine Learning*. Springer, New York, 2006.

Alexander Black, Simon Jenni, Tu Bui, Md. Mehrab Tanjim, Stefano Petrangeli, Ritwik Sinha, Viswanathan Swaminathan, and John Collomosse. Vader: Video alignment differencing and retrieval, 2023. URL `https://arxiv.org/abs/2303.13193`.

Tolga Bolukbasi, Kai-Wei Chang, James Y Zou, Venkatesh Saligrama, and Adam T Kalai. Man is to computer programmer as woman is to homemaker? debiasing word embeddings. *Advances in neural information processing systems*, 29, 2016.

John S. Bridle. Training stochastic model recognition algorithms as networks can lead to maximum mutual information estimation of parameters. In *Advances in Neural Information Processing Systems*, volume 2, pp. 211–217. Morgan Kaufmann, 1990.

Haoxin Chen, Menghan Xia, Yingqing He, Yong Zhang, Xiaodong Cun, Shaoshu Yang, Jinbo Xing, Yaofang Liu, Qifeng Chen, Xintao Wang, et al. Videocrafter1: Open diffusion models for high-quality video generation. *arXiv preprint arXiv:2310.19512*, 2023.

Haoxin Chen, Yong Zhang, Xiaodong Cun, Menghan Xia, Xintao Wang, Chao Weng, and Ying Shan. Videocrafter2: Overcoming data limitations for high-quality video diffusion models, 2024a. URL `https://arxiv.org/abs/2401.09047`.

Zhe Chen, Weiyun Wang, Yue Cao, Yangzhou Liu, Zhangwei Gao, Erfei Cui, Jinguo Zhu, Shenglong Ye, Hao Tian, Zhaoyang Liu, et al. Expanding performance boundaries of open-source multimodal models with model, data, and test-time scaling. *arXiv preprint arXiv:2412.05271*, 2024b.

Jaemin Cho, Abhay Zala, and Mohit Bansal. Dall-eval: Probing the reasoning skills and social biases of text-to-image generation models. In *Proceedings of the IEEE/CVF International Conference on Computer Vision*, pp. 3043–3054, 2023.

Joseph Cho, Samuel Schmidgall, Cyril Zakka, Mrudang Mathur, Dhamanpreet Kaur, Rohan Shad, and William Hiesinger. Surgen: Text-guided diffusion model for surgical video generation. *arXiv preprint arXiv:2408.14028*, 2024.

Michael Feldman, Sorelle A. Friedler, John Moeller, Carlos Scheidegger, and Suresh Venkatasubramanian. Certifying and removing disparate impact. In *Proceedings of the 21th ACM SIGKDD International Conference on Knowledge Discovery and Data Mining (KDD)*, pp. 259–268. ACM, 2015.

Nikhil Garg, Londa Schiebinger, Dan Jurafsky, and James Zou. Word embeddings quantify 100 years of gender and ethnic stereotypes. *Proceedings of the National Academy of Sciences*, 115(16):E3635–E3644, 2018.

Lisa Anne Hendricks and Aida Nematzadeh. Probing image-language transformers for verb understanding. *arXiv preprint arXiv:2106.09141*, 2021.

Jack Hessel, Ari Holtzman, Maxwell Forbes, Ronan Le Bras, and Yejin Choi. Clipscore: A reference-free evaluation metric for image captioning. *arXiv preprint arXiv:2104.08718*, 2021.

Phillip Howard, Avinash Madasu, Tiep Le, Gustavo Lujan Moreno, Anahita Bhiwandiwalla, and Vasudev Lal. Socialcounterfactuals: Probing and mitigating intersectional social biases in vision-language models with counterfactual examples. In *Proceedings of the IEEE/CVF Conference on Computer Vision and Pattern Recognition*, pp. 11975–11985, 2024.

Ziqi Huang, Yinan He, Jiashuo Yu, Fan Zhang, Chenyang Si, Yuming Jiang, Yuanhan Zhang, Tianxing Wu, Qingyang Jin, Nattapol Chanpaisit, et al. Vbench: Comprehensive benchmark suite for video generative models. In *Proceedings of the IEEE/CVF Conference on Computer Vision and Pattern Recognition*, pp. 21807–21818, 2024.

Kimmo Karkkainen and Jungseock Joo. Fairface: Face attribute dataset for balanced race, gender, and age for bias measurement and mitigation. In *Proceedings of the IEEE/CVF winter conference on applications of computer vision*, pp. 1548–1558, 2021.

Yuval Kirstain, Adam Polyak, Uriel Singer, Shahbuland Matiana, Joe Penna, and Omer Levy. Pick-a-pic: An open dataset of user preferences for text-to-image generation. 2023a.

Yuval Kirstain, Adam Polyak, Uriel Singer, Shahbuland Matiana, Joe Penna, and Omer Levy. Pick-a-pic: An open dataset of user preferences for text-to-image generation. *Advances in Neural Information Processing Systems*, 36:36652–36663, 2023b.

Black Forest Labs. Flux. https://github.com/black-forest-labs/flux, 2023.

Jiachen Li, Weixi Feng, Tsu-Jui Fu, Xinyi Wang, Sugato Basu, Wenhu Chen, and William Yang Wang. T2v-turbo: Breaking the quality bottleneck of video consistency model with mixed reward feedback. *arXiv preprint arXiv:2405.18750*, 2024.

Runtao Liu, Haoyu Wu, Zheng Ziqiang, Chen Wei, Yingqing He, Renjie Pi, and Qifeng Chen. Videodpo: Omni-preference alignment for video diffusion generation. *arXiv preprint arXiv:2412.14167*, 2024a.

Yaofang Liu, Xiaodong Cun, Xuebo Liu, Xintao Wang, Yong Zhang, Haoxin Chen, Yang Liu, Tieyong Zeng, Raymond Chan, and Ying Shan. Evalcrafter: Benchmarking and evaluating large video generation models. In *Proceedings of the IEEE/CVF Conference on Computer Vision and Pattern Recognition*, pp. 22139–22149, 2024b.

Alexandra Sasha Luccioni, Christopher Akiki, Margaret Mitchell, and Yacine Jernite. Stable bias: Analyzing societal representations in diffusion models. *arXiv preprint arXiv:2303.11408*, 2023.

Simian Luo, Yiqin Tan, Longbo Huang, Jian Li, and Hang Zhao. Latent consistency models: Synthesizing high-resolution images with few-step inference, 2023. URL https://arxiv.org/abs/2310.04378.

Guoqing Ma, Haoyang Huang, Kun Yan, Liangyu Chen, Nan Duan, Shengming Yin, Changyi Wan, Ranchen Ming, Xiaoniu Song, Xing Chen, Yu Zhou, Deshan Sun, Deyu Zhou, Jian Zhou, Kaijun Tan, Kang An, Mei Chen, Wei Ji, Qiling Wu, Wen Sun, Xin Han, Yanan Wei, Zheng Ge, Aojie Li, Bin Wang, Bizhu Huang, Bo Wang, Brian Li, Changxing Miao, Chen Xu, Chenfei Wu, Chenguang Yu, Dapeng Shi, Dingyuan Hu, Enle Liu, Gang Yu, Ge Yang, Guanzhe Huang, Gulin Yan, Haiyang Feng, Hao Nie, Haonan Jia, Hanpeng Hu, Hanqi Chen, Haolong Yan, Heng Wang, Hongcheng Guo, Huilin Xiong, Huixin Xiong, Jiahao Gong, Jianchang Wu, Jiaoren Wu, Jie Wu, Jie Yang, Jiashuai Liu, Jiashuo Li, Jingyang Zhang, Junjing Guo, Junzhe Lin, Kaixiang Li, Lei Liu, Lei Xia, Liang Zhao, Liguo Tan, Liwen Huang, Liying Shi, Ming Li, Mingliang Li, Muhua Cheng, Na Wang, Qiaohui Chen, Qinglin He, Qiuyan Liang, Quan Sun, Ran Sun, Rui Wang, Shaoliang Pang, Shiliang Yang, Sitong Liu, Siqi Liu, Shuli Gao, Tiancheng Cao, Tianyu Wang, Weipeng Ming, Wenqing He, Xu Zhao, Xuelin Zhang, Xianfang Zeng, Xiaojia Liu, Xuan Yang, Yaqi Dai, Yanbo Yu, Yang Li, Yineng Deng, Yingming Wang, Yilei Wang, Yuanwei Lu, Yu Chen, Yu Luo, Yuchu Luo, Yuhe Yin, Yuheng Feng, Yuxiang Yang, Zecheng Tang, Zekai Zhang, Zidong Yang, Binxing Jiao, Jiansheng Chen, Jing Li, Shuchang Zhou, Xiangyu Zhang, Xinhao Zhang, Yibo Zhu, Heung-Yeung Shum, and Daxin Jiang. Step-video-t2v technical report: The practice, challenges, and future of video foundation model, 2025. URL https://arxiv.org/abs/2502.10248.

Ninareh Mehrabi, Fred Morstatter, Nripsuta Saxena, Kristina Lerman, and Aram Galstyan. A survey on bias and fairness in machine learning. *ACM Computing Surveys (CSUR)*, 54(6):1–35, 2021.

Elijah Miller, Thomas Dupont, and Mingming Wang. Enhanced creativity and ideation through stable video synthesis. *arXiv preprint arXiv:2405.13357*, 2024.

Mihir Prabhudesai, Russell Mendonca, Zheyang Qin, Katerina Fragkiadaki, and Deepak Pathak. Video diffusion alignment via reward gradients. *arXiv preprint arXiv:2407.08737*, 2024.

Haoyi Qiu, Zi-Yi Dou, Tianlu Wang, Asli Celikyilmaz, and Nanyun Peng. Gender biases in automatic evaluation metrics for image captioning. *arXiv preprint arXiv:2305.14711*, 2023.

Haoyi Qiu, Alexander R Fabbri, Divyansh Agarwal, Kung-Hsiang Huang, Sarah Tan, Nanyun Peng, and Chien-Sheng Wu. Evaluating cultural and social awareness of llm web agents. *arXiv preprint arXiv:2410.23252*, 2024a.

Haoyi Qiu, Wenbo Hu, Zi-Yi Dou, and Nanyun Peng. Valor-eval: Holistic coverage and faithfulness evaluation of large vision-language models. *arXiv preprint arXiv:2404.13874*, 2024b.

Haoyi Qiu, Kung-Hsiang Huang, Ruichen Zheng, Jiao Sun, and Nanyun Peng. Multimodal cultural safety: Evaluation frameworks and alignment strategies. *arXiv preprint arXiv:2505.14972*, 2025.

Alec Radford, Jong Wook Kim, Chris Hallacy, Aditya Ramesh, Gabriel Goh, Sandhini Agarwal, Girish Sastry, Amanda Askell, Pamela Mishkin, Jack Clark, et al. Learning transferable visual models from natural language supervision. In *International conference on machine learning*, pp. 8748–8763. PMLR, 2021.

Xudong Shen, Chao Du, Tianyu Pang, Min Lin, Yongkang Wong, and Mohan Kankanhalli. Finetuning text-to-image diffusion models for fairness. *arXiv preprint arXiv:2311.07604*, 2023.

Emily Sheng, Kai-Wei Chang, Premkumar Natarajan, and Nanyun Peng. Towards controllable biases in language generation. *arXiv preprint arXiv:2005.00268*, 2020.

Edward H Simpson. Measurement of diversity. *Nature*, 163(4148):688–688, 1949.

Jiao Sun and Nanyun Peng. Men are elected, women are married: Events gender bias on Wikipedia. In Chengqing Zong, Fei Xia, Wenjie Li, and Roberto Navigli (eds.), *Proceedings of the 59th Annual Meeting of the Association for Computational Linguistics and the 11th International Joint Conference on Natural Language Processing (Volume 2: Short Papers)*, pp. 350–360, Online, August 2021. Association for Computational Linguistics. doi: 10.18653/v1/2021.acl-short.45. URL `https://aclanthology.org/2021.acl-short.45/`.

Kaiyue Sun, Kaiyi Huang, Xian Liu, Yue Wu, Zihan Xu, Zhenguo Li, and Xihui Liu. T2v-compbench: A comprehensive benchmark for compositional text-to-video generation. *arXiv preprint arXiv:2407.14505*, 2024.

Thomas Unterthiner, Sjoerd Van Steenkiste, Karol Kurach, Raphaël Marinier, Marcin Michalski, and Sylvain Gelly. Fvd: A new metric for video generation. 2019.

Jiuniu Wang, Hangjie Yuan, Dayou Chen, Yingya Zhang, Xiang Wang, and Shiwei Zhang. Modelscope text-to-video technical report. *arXiv preprint arXiv:2308.06571*, 2023a.

Peng Wang, Shuai Bai, Sinan Tan, Shijie Wang, Zhihao Fan, Jinze Bai, Keqin Chen, Xuejing Liu, Jialin Wang, Wenbin Ge, et al. Qwen2-vl: Enhancing vision-language model's perception of the world at any resolution. *arXiv preprint arXiv:2409.12191*, 2024a.

Yi Wang, Yinan He, Yizhuo Li, Kunchang Li, Jiashuo Yu, Xin Ma, Xinhao Li, Guo Chen, Xinyuan Chen, Yaohui Wang, et al. Internvid: A large-scale video-text dataset for multimodal understanding and generation. *arXiv preprint arXiv:2307.06942*, 2023b.

Yi Wang, Kunchang Li, Xinhao Li, Jiashuo Yu, Yinan He, Guo Chen, Baoqi Pei, Rongkun Zheng, Jilan Xu, Zun Wang, et al. Internvideo2: Scaling video foundation models for multimodal video understanding. *arXiv preprint arXiv:2403.15377*, 2024b.

Jialian Wu, Jianfeng Wang, Zhengyuan Yang, Zhe Gan, Zicheng Liu, Junsong Yuan, and Lijuan Wang. Grit: A generative region-to-text transformer for object understanding. In *European Conference on Computer Vision*, pp. 207–224. Springer, 2025.

Xiaoshi Wu, Yiming Hao, Keqiang Sun, Yixiong Chen, Feng Zhu, Rui Zhao, and Hongsheng Li. Human preference score v2: A solid benchmark for evaluating human preferences of text-to-image synthesis. *arXiv preprint arXiv:2306.09341*, 2023.

Jiazheng Xu, Xiao Liu, Yuchen Wu, Yuxuan Tong, Qinkai Li, Ming Ding, Jie Tang, and Yuxiao Dong. Imagereward: Learning and evaluating human preferences for text-to-image generation. *Advances in Neural Information Processing Systems*, 36, 2024.

An Yang, Baosong Yang, Beichen Zhang, Binyuan Hui, Bo Zheng, Bowen Yu, Chengyuan Li, Dayiheng Liu, Fei Huang, Haoran Wei, et al. Qwen2. 5 technical report. *arXiv preprint arXiv:2412.15115*, 2024.

Da Yin, Haoyi Qiu, Kung-Hsiang Huang, Kai-Wei Chang, and Nanyun Peng. Safeworld: Geo-diverse safety alignment. *Advances in Neural Information Processing Systems*, 37:128734–128768, 2024.

Hangjie Yuan, Shiwei Zhang, Xiang Wang, Yujie Wei, Tao Feng, Yining Pan, Yingya Zhang, Ziwei Liu, Samuel Albanie, and Dong Ni. Instructvideo: instructing video diffusion models with human feedback. In *Proceedings of the IEEE/CVF Conference on Computer Vision and Pattern Recognition*, pp. 6463–6474, 2024.

Mike Zajko. Conservative ai and social inequality: conceptualizing alternatives to bias through social theory. *Ai & Society*, 36(3):1047–1056, 2021.

Jieyu Zhao, Tianlu Wang, Mark Yatskar, Vicente Ordonez, and Kai-Wei Chang. Men also like shopping: Reducing gender bias amplification using corpus-level constraints. *arXiv preprint arXiv:1707.09457*, 2017.

A Social Biases in Video Generative Models

To demonstrate the utility of our framework, we apply it to *four* state-of-the-art video diffusion models with varying alignment strategies. The **aligned** models include InstructVideo Yuan et al. (2024), which is based on ModelScope Wang et al. (2023a) and aligned with HPSv2.0, and T2V-Turbo-V1 Li et al. (2024), which builds on VideoCrafter-2 Chen et al. (2024a) and is aligned with HPSv2.1, InternVid2-S2 Wang et al. (2024b), and ViCLIP Wang et al. (2023b). Their **unaligned** counterparts, ModelScope and VideoCrafter-2, serve as baselines for controlled comparisons. For implementation, we use the official code repositories provided by the respective papers and run inference on 1 to 8 NVIDIA A100 80GB GPUs. To compute the social bias distribution, as outlined in §3, we generate videos with each prompt 10 times per model with different random seeds and average the results to reduce sampling variance. Table 2 reports two social bias metrics: ethnicity-aware gender bias (PBS_G) and ethnic representation distribution (RDS_e and SDI).

Ethnicity-Aware Gender Bias. We evaluate gender portrayals under the `ethnicity+person` condition using the previously defined PBS_G metric. All models exhibit a consistent male bias, with average PBS_G values remaining above zero across all ethnic groups. Moreover, *alignment tuning amplifies this imbalance*: InstructVideo and T2V-Turbo-V1 show PBS_G increases of 0.04 and 0.0725, respectively, indicating that preference-based fine-tuning may worsen gender disparity rather than alleviate it. Figures 5 to 11 presents the PBS_G scores across 42 actions for each ethnicity group in {White, Black, Indian, East Asian, Southeast Asian, Middle Eastern, Latino}.

Ethnicity Bias. Under the `ethnicity-only` condition, we analyze models' representation balance using the previously defined RDS_e and SDI metrics. All models show a pronounced overrepresentation of White individuals, though the magnitude varies. ModelScope exhibits the strongest imbalance ($\text{RDS}_\text{White} = 0.769$, $\text{SDI} = 0.0538$), which is further amplified by alignment tuning in InstructVideo ($\text{RDS}_\text{White} = 0.783$, $\text{SDI} = 0.0267$). VideoCrafter-2 achieves moderately improved balance ($\text{RDS}_\text{White} = 0.6905$, $\text{SDI} = 0.1252$), while T2V-Turbo-V1 further reduces White dominance ($\text{RDS}_\text{White} = 0.6381$) but at the cost of lower diversity ($\text{SDI} = 0.1119$). Overall, while alignment tuning may alleviate certain ethnic skews, it can also suppress demographic diversity, suggesting a trade-off between bias reduction and representational variety. Figure 12 show the ethnicity bias across 42 actions.

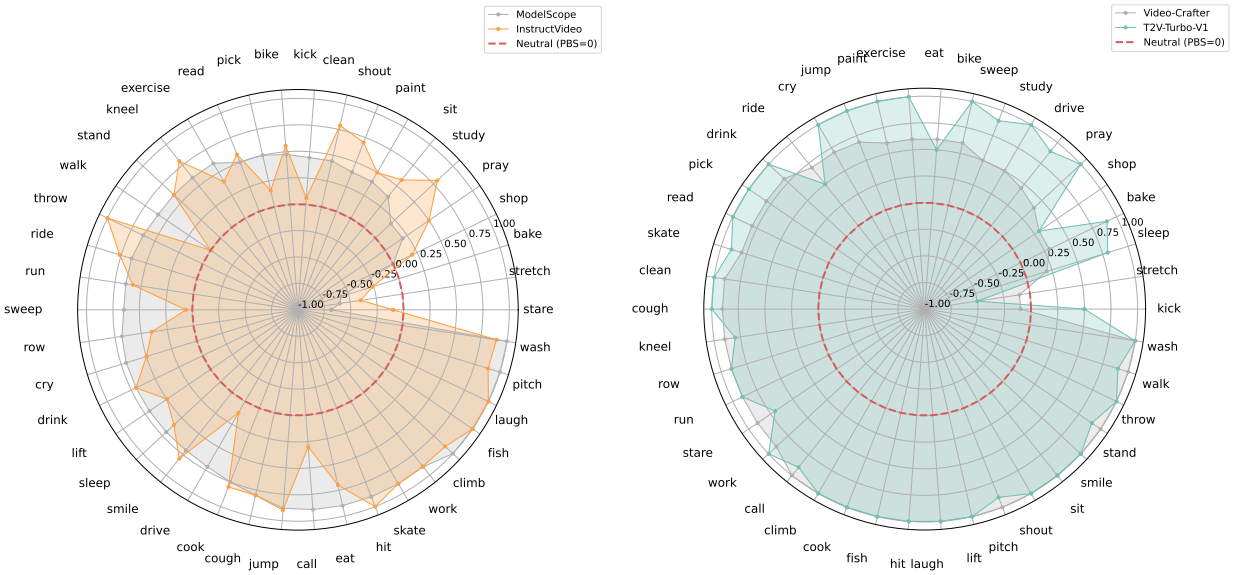

(a) ModelScope vs. InstructVideo

(b) Video-Crafter-2 vs. T2V-Turbo-V1

Figure 5: Ethnicity-aware gender bias (White).

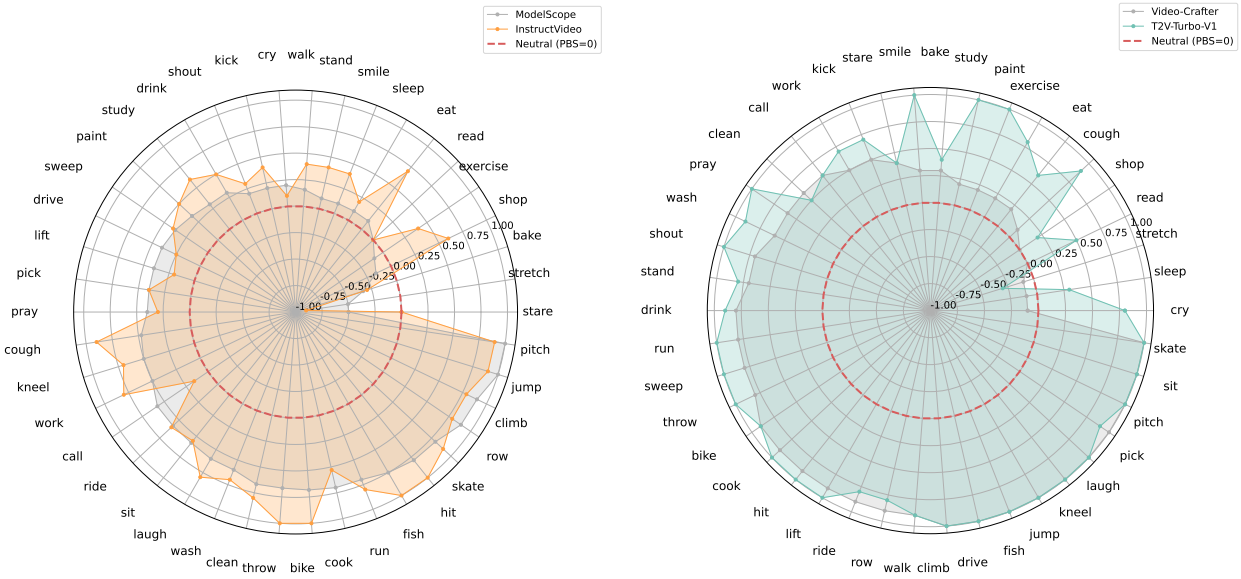

(a) ModelScope vs. InstructVideo

(b) Video-Crafter-2 vs. T2V-Turbo-V1

Figure 6: Ethnicity-aware gender bias (Black).

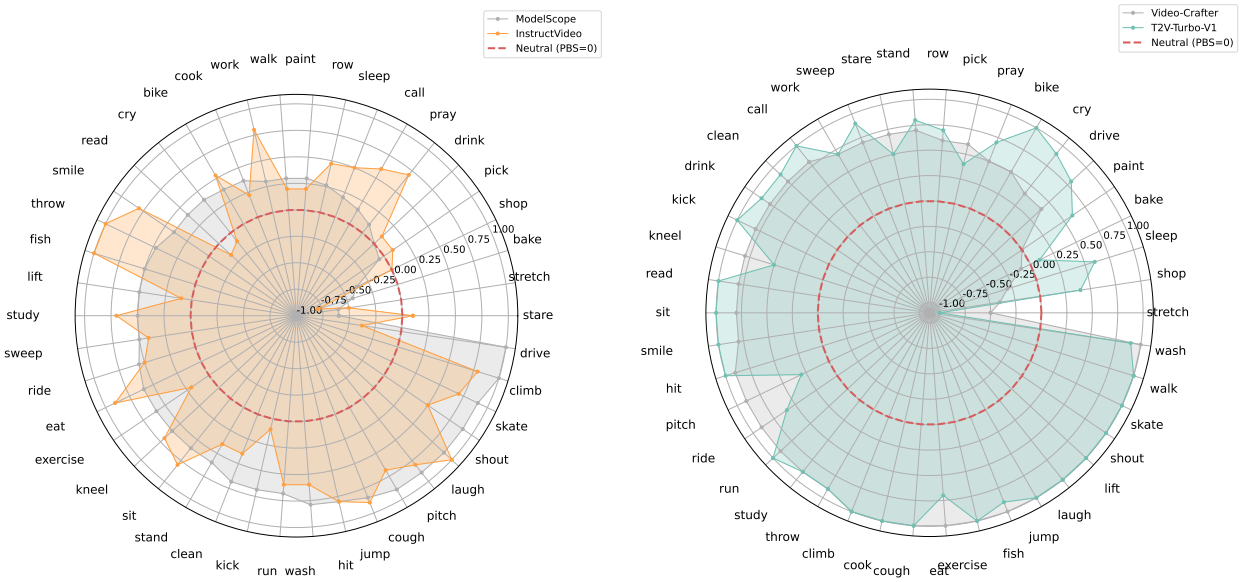

(a) ModelScope vs. InstructVideo (orange)

(b) Video-Crafter-2 vs. T2V-Turbo-V1

Figure 7: Ethnicity-aware gender bias (East Asian).

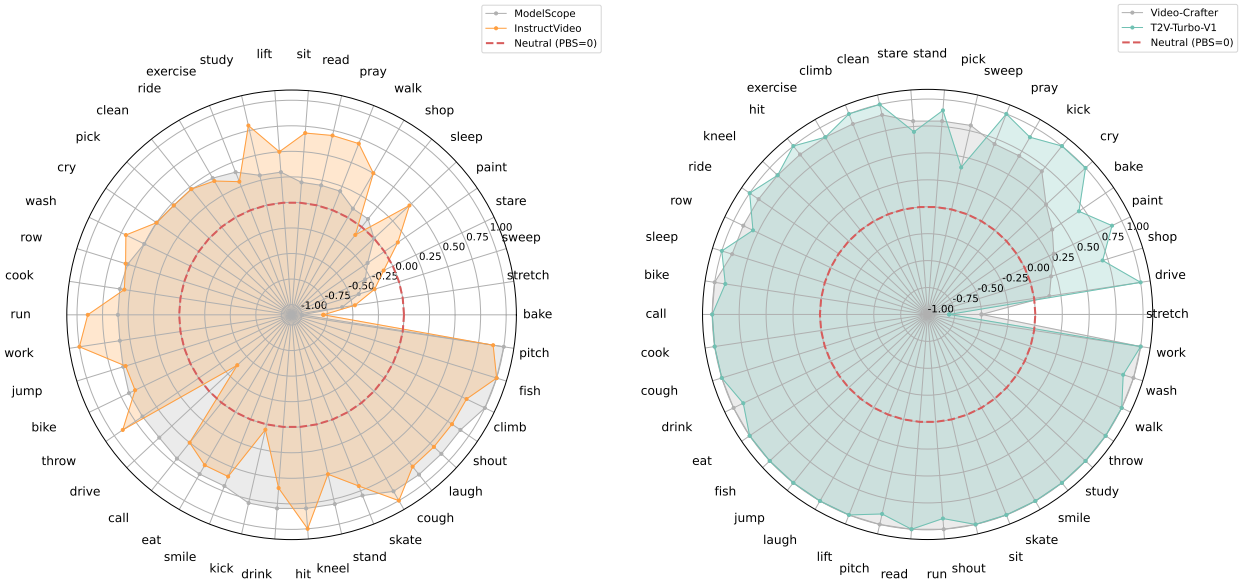

(a) ModelScope vs. InstructVideo

(b) Video-Crafter-2 vs. T2V-Turbo-V1

Figure 8: Ethnicity-aware gender bias (Southeast Asian).

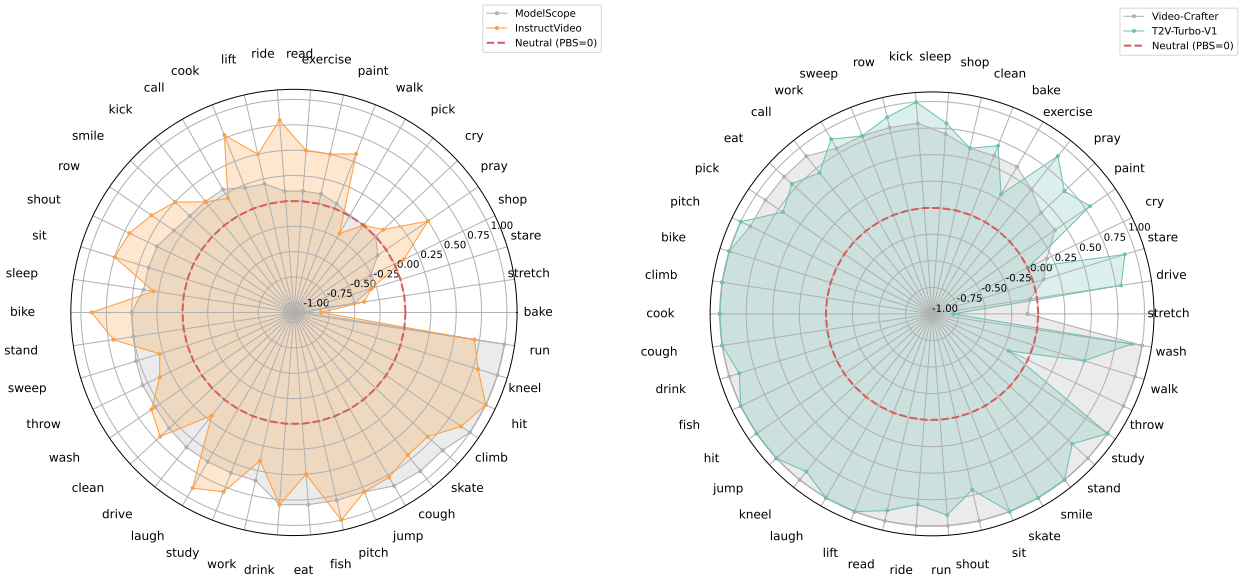

(a) ModelScope vs. InstructVideo

(b) Video-Crafter-2 vs. T2V-Turbo-V1

Figure 9: Ethnicity-aware gender bias (Indian).

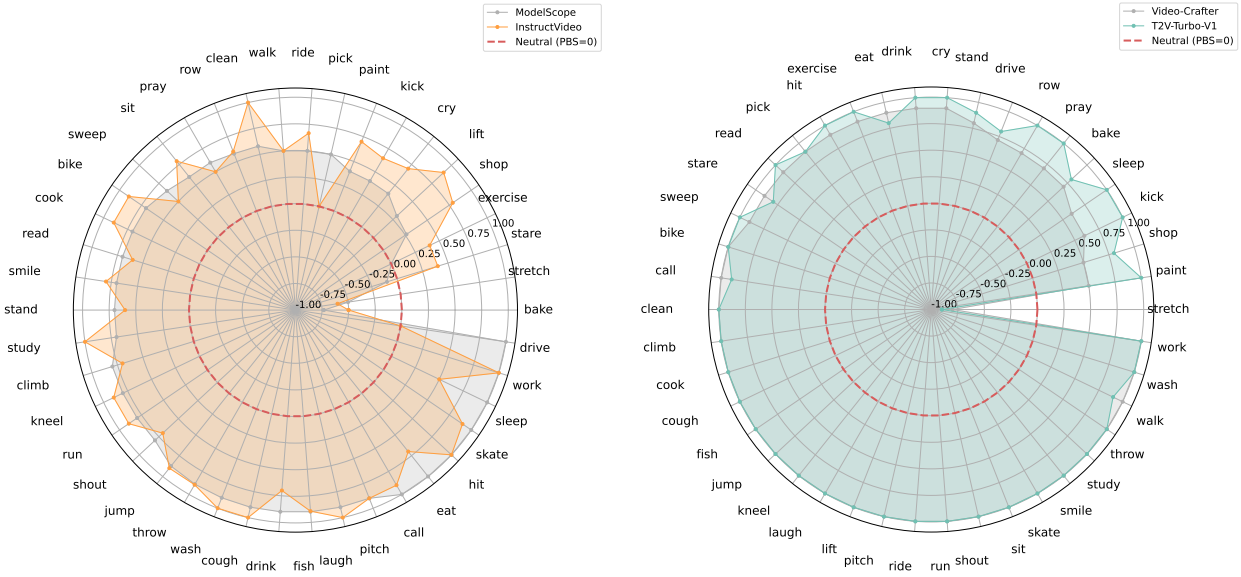

(a) ModelScope vs. InstructVideo

(b) Video-Crafter-2 vs. T2V-Turbo-V1

Figure 10: Ethnicity-aware gender bias (Latino).

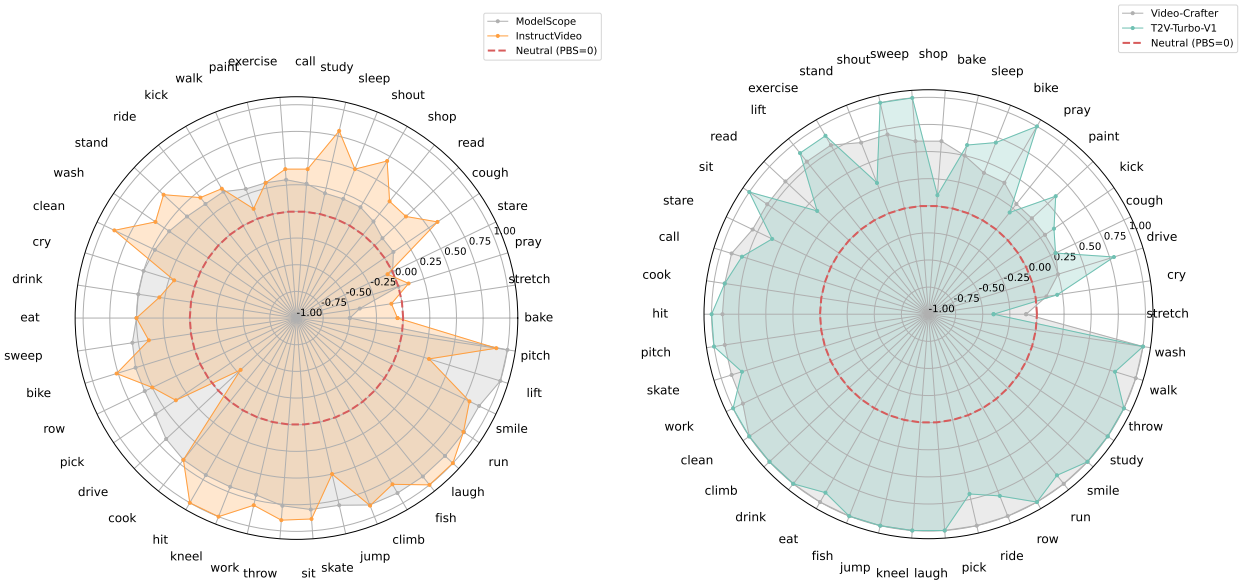

(a) ModelScope vs. InstructVideo

(b) Video-Crafter-2 vs. T2V-Turbo-V1

Figure 11: Ethnicity-aware gender bias (Middle Eastern).

Figure 12: Ethnicity bias distribution.

B Social Biases in Image Reward Datasets

We analyze *two* widely used image reward datasets to investigate preference biases: HPDv2 Wu et al. (2023) and Pick-a-Pic Kirstain et al. (2023b). For each dataset, we extract gender, ethnicity, and action attributes from image captions using GPT-4o-mini, and classify attributes from images using three VLMs (Qwen2-VL-7B, Qwen2.5-VL-7B, InternVL2.5-8B). We then aggregate the social attributes from both caption and image modalities, retaining only instances featuring one of our predefined actions. After processing, HPDv2 contains 28,783 validated (images, caption, preference) tuples covering 29 actions, and Pick-a-Pic contains 14,958 across 19 actions. Each tuple presents two images, with a human annotator selecting the one that best matches the caption. To assess potential preference biases, we measure how often annotators *prefer* specific gender or ethnicity representations for given actions.

Figure 13 shows the gender preference bias across 42 actions in the two datasets. Values greater than zero (outside the red circle) indicate a man-preferred bias, while values less than zero (inside the red circle) indicate a woman-preferred bias. Points on the red circle represent more neutral preference. In **HPDv2**, 62.07% (18/29) of actions show a preference for men, while only 24.14% (7/29) favor women, indicating a skew toward **man-preferred** representations. In contrast, **Pick-a-Pic** reveals a **woman-preferred** tendency, with 57.89% (11/19) of actions biased toward women and 26.32% (5/19) toward men. These patterns highlight that both datasets exhibit non-neutral gender preferences, though in opposing directions, potentially shaping downstream alignment in different ways.

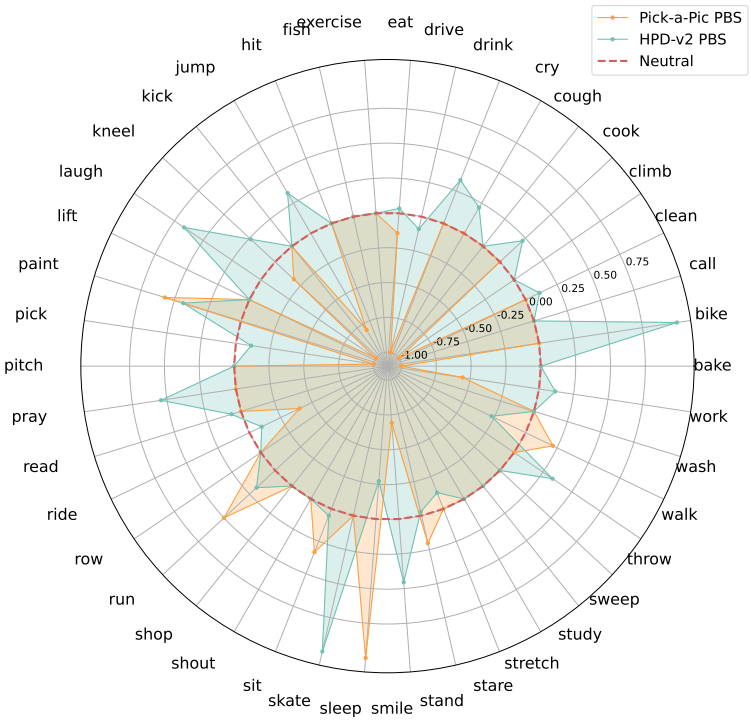

Figure 13: Image reward datasets gender preference distribution.

Table 9 presents the ethnicity preference distribution across the two image reward datasets, while Figure 14 provides a fine-grained breakdown across 42 actions. Notably, both datasets exhibit a strong preference for the **White** group, 43.34% in HPDv2 and 40.08% in Pick-a-Pic, followed by East Asian and Indian representations. Despite certain actions showing distinct preferences (*e.g.*, "bake" favoring Black individuals and "fish" favoring East Asians), the overall distributions reveal a pronounced imbalance skewed toward White representations. This suggests that the reward signals used to guide image generation may reflect and reinforce ethnic biases embedded in the datasets. This imbalance in collected preferences risks might propagate representational bias during reward model training, ultimately reinforcing societal inequities in

downstream video generation. These findings underscore the urgent need for more inclusive and representative datasets that reflect global demographic diversity in both identity and activity contexts.

Datasets	White	Black	Latino	East Asian	Southeast Asian	India	Middle Eastern
HPDv2	43.34	9.16	4.44	19.38	1.39	20.20	2.09
Pick-a-Pic	40.08	15.36	8.51	19.94	0.20	13.34	2.56

Table 9: Ethnicity distribution across reward datasets (in %).

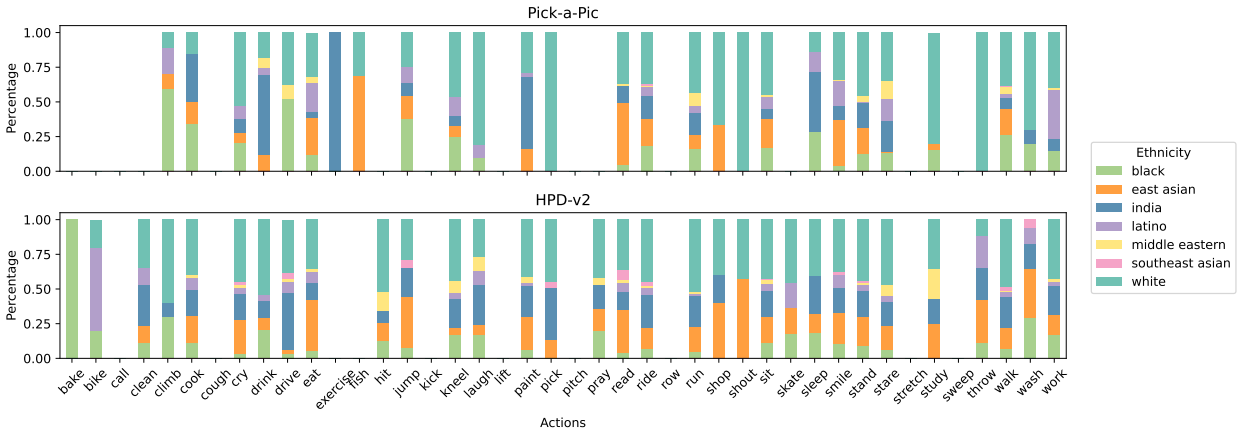

Figure 14: Ethnicity preference distribution across 42 actions.

C Social Biases in Image Reward Models

Preference Bias Evaluation. To systematically evaluate social biases in reward models, we construct a controlled benchmark based on text-to-image (T2I) generation, inspired by HPDv2 (Wu et al., 2023) and ImageRewardDB (Xu et al., 2024). Using the event prompting templates introduced in Section 3.2, we employ FLUX (Labs, 2023), a state-of-the-art T2I model, to generate diverse image sets varying systematically across gender, ethnicity, and action dimensions. The benchmark includes two evaluation settings: (1) `Ethnicity+Person`, where prompts specify only the actor's ethnicity, and (2) `Ethnicity+Gender`, where both gender and ethnicity are explicitly indicated. Table 3 summarizes prompt coverage and provides representative examples. To ensure statistical robustness, we generate 100 images per prompt, resulting in a large and diverse evaluation set. Sample outputs are illustrated in Figure 3.

Ethnicity-Aware Gender Bias. We construct preference evaluation prompts in the format "A/An `[ethnicity]` person is `[action]`-ing `[context]`", covering all combinations of ethnicity and action, resulting in $|E| \times |A|$ evaluation prompts. For each preference prompt, we generate images using generation prompts in the format "A/An `[ethnicity]` `[gender]` is `[action]`-ing `[context]`", where gender, ethnicity, and action are explicitly specified. This yields a total of $|G| \times |E| \times |A| \times 100$ images. The reward scores assigned to these images by a reward model are standardized using their mean and standard deviation. We then compute the average standardized score across the 100 images for each generation prompt, resulting in $|G| \times |E| \times |A|$ mean scores. To compute the final PBS_G, we fix the ethnicity and action, and subtract the average standardized score for women from that for men, producing $|E| \times |A|$ PBS_G values.

A positive PBS_G score indicates a preference for men, while a negative score reflects a preference for women. The base reward model, CLIP, exhibits a mild woman-preference bias overall ($\text{PBS}_\text{G} = -0.0726$). After fine-tuning on HPDv2, HPSv2.0 reverses this trend and demonstrates a notable shift toward man-preference bias (+0.6039), consistent across most ethnic groups. In contrast, PickScore shows a stronger woman-preference bias ($\text{PBS}_\text{G} = -0.1157$), aligning with the characteristics of Pick-a-Pic. HPSv2.1 also exhibits a

woman-preference trend (PBS_G = –0.0984), though its training data has not been publicly disclosed. These directional shifts are evident across all ethnic groups, suggesting that model fine-tuning introduces consistent and dataset-aligned gender preferences. Figures 15 to 21 presents the PBS_G scores across 42 actions for each ethnicity group.

Ethnicity Bias. We use preference evaluation prompts in the form "A person is `[action]`-ing `[context]`", covering all actions and resulting in $|A|$ evaluation prompts. For each preference prompt, we have generated images using more specific generation prompts of the form "A/An `[ethnicity]` person is `[action]`-ing `[context]`", where the ethnicity and action are explicitly specified. For each such combination, we have a total of $|E| \times |A| \times 100$ images. The reward scores for these images provided by a reward model are standardized with mean and standard deviation. We then compute the average standardized score across the 100 images for each generation prompt, leading to $|E| \times |A|$ mean scores. To calculate RDS_e and SDI, we fix the action and apply softmax function Bridle (1990); Bishop (2006) to normalize the scores for each ethnicity. This results in $|E| \times |A|$ final RDS_e scores and $|A|$ SDI scores, indicating ethnicity preference within each action context.

A positive RDS_e score indicates overrepresentation of a specific ethnicity group, while a negative score reflects underrepresentation. A higher SDI score corresponds to more balanced and diverse outputs across all groups. The base reward model, CLIP, shows a mild overrepresentation of the White group (RDS = 0.0182) and achieves the highest SDI score (0.8495), indicating relatively balanced ethnic representation. After fine-tuning, HPSv2.0 shifts its preference toward Middle Eastern individuals (RDS = 0.0315), while HPSv2.1 displays a stronger bias toward the Latino group (RDS = 0.0382). PickScore, by contrast, favors East Asian individuals (RDS = 0.0352). Despite differences in the direction of bias, all fine-tuned reward models exhibit lower SDI scores compared to CLIP, suggesting a decline in ethnic diversity and balance following alignment. Figures 22 to 25 show the ethnicity bias across 42 actions.

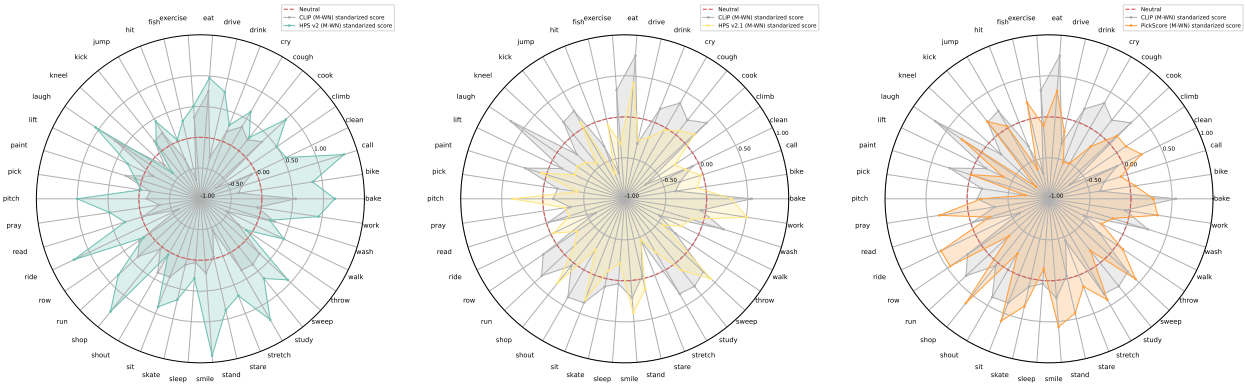

(a) HPSv2.0 vs. CLIP (b) HPSv2.1 vs. CLIP (c) PickScore vs. CLIP

Figure 15: Ethnicity-aware gender bias (White).

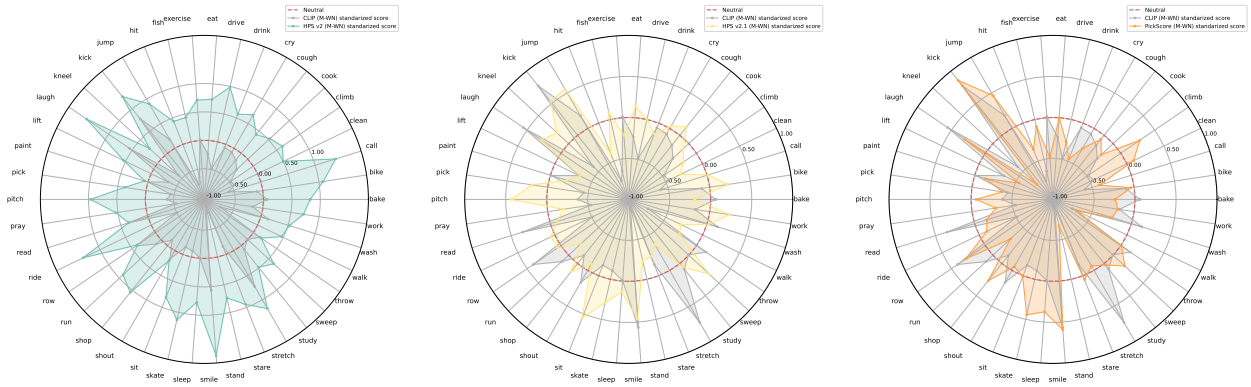

(a) HPSv2.0 vs. CLIP (b) HPSv2.1 vs. CLIP (c) PickScore vs. CLIP

Figure 16: Ethnicity-aware gender bias (Black).

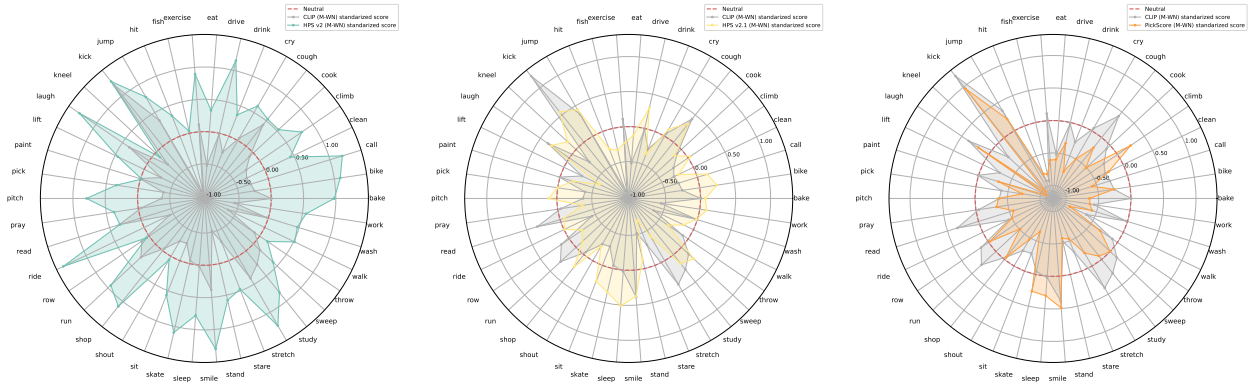

(a) HPSv2.0 vs. CLIP (b) HPSv2.1 vs. CLIP (c) PickScore vs. CLIP

Figure 17: Ethnicity-aware gender bias (Latino).

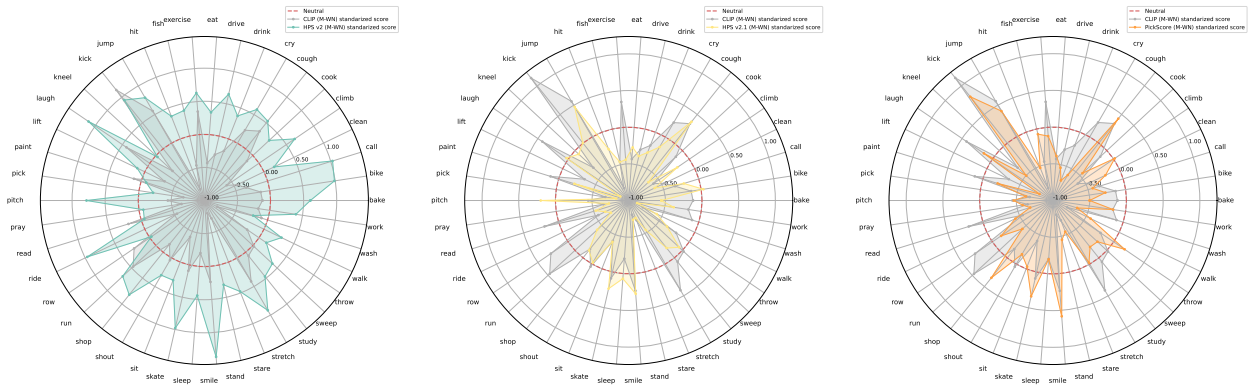

(a) HPSv2.0 vs. CLIP (b) HPSv2.1 vs. CLIP (c) PickScore vs. CLIP

Figure 18: Ethnicity-aware gender bias (East Asian).

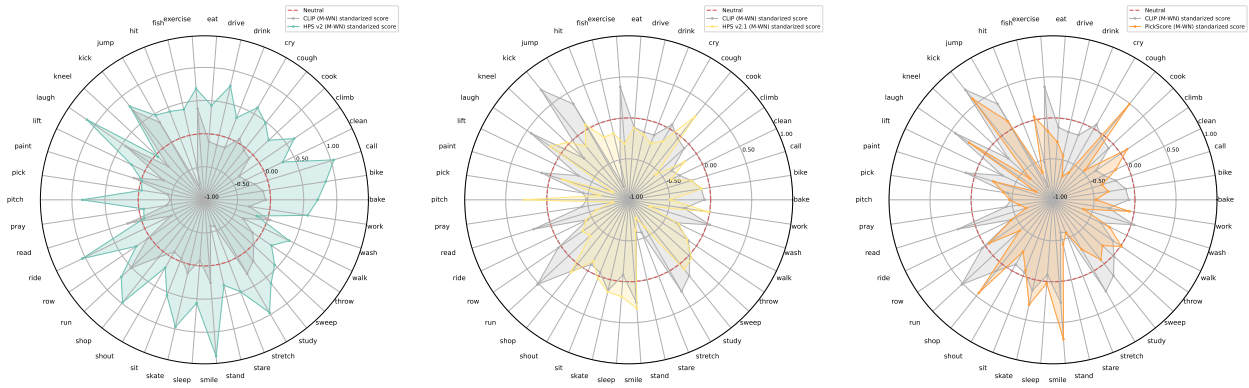

(a) HPSv2.0 vs. CLIP (b) HPSv2.1 vs. CLIP (c) PickScore vs. CLIP

Figure 19: Ethnicity-aware gender bias (Southeast Asian).

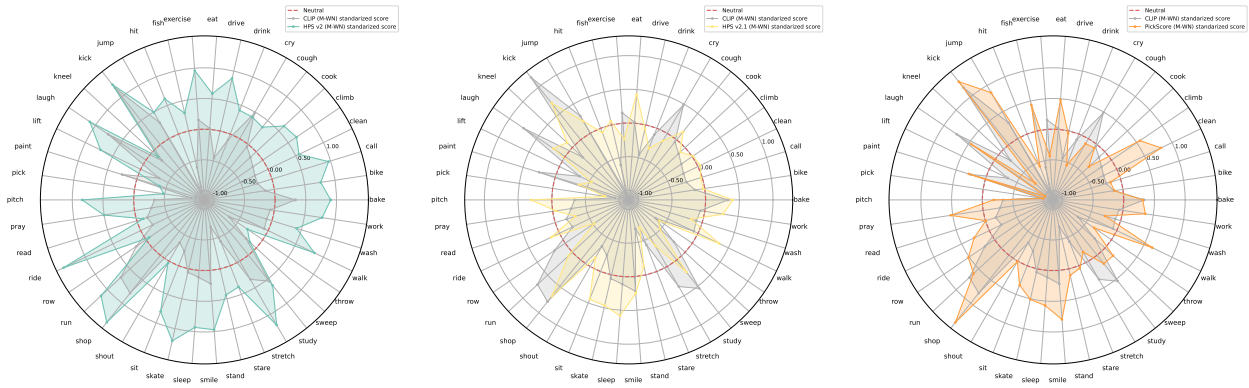

(a) HPSv2.0 vs. CLIP (b) HPSv2.1 vs. CLIP (c) PickScore vs. CLIP

Figure 20: Ethnicity-aware gender bias (Indian).

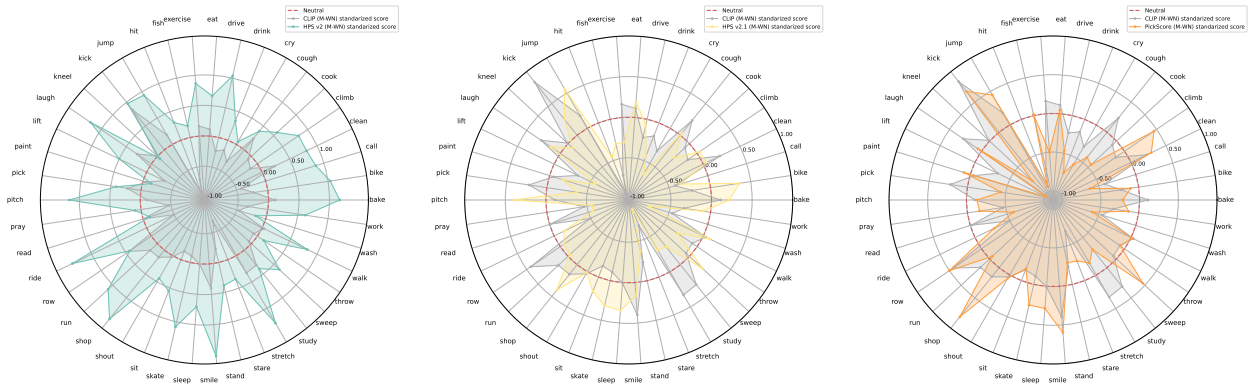

(a) HPSv2.0 vs. CLIP (b) HPSv2.1 vs. CLIP (c) PickScore vs. CLIP

Figure 21: Ethnicity-aware gender bias (Middle Eastern).

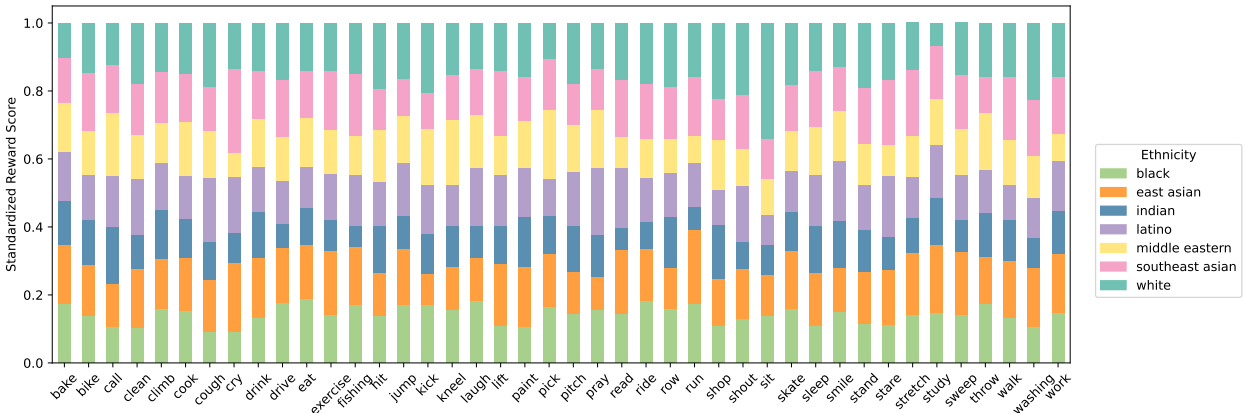

Figure 22: Ethnicity Bias - CLIP

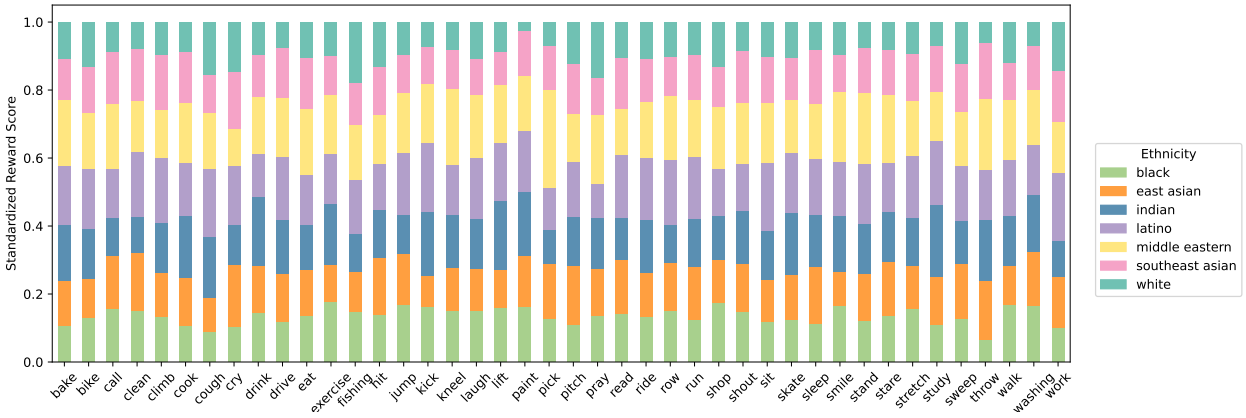

Figure 23: Ethnicity Bias - HPSv2.0

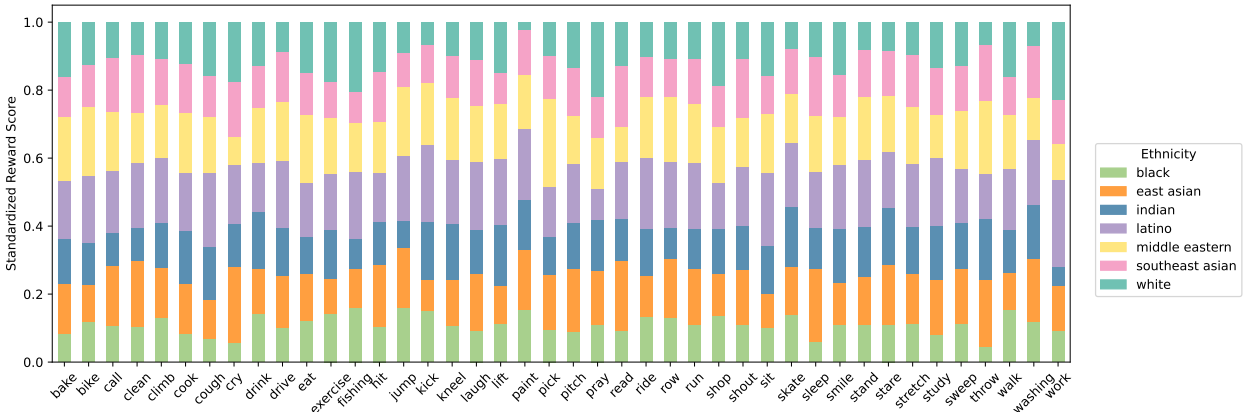

Figure 24: Ethnicity Bias - HPSv2.1

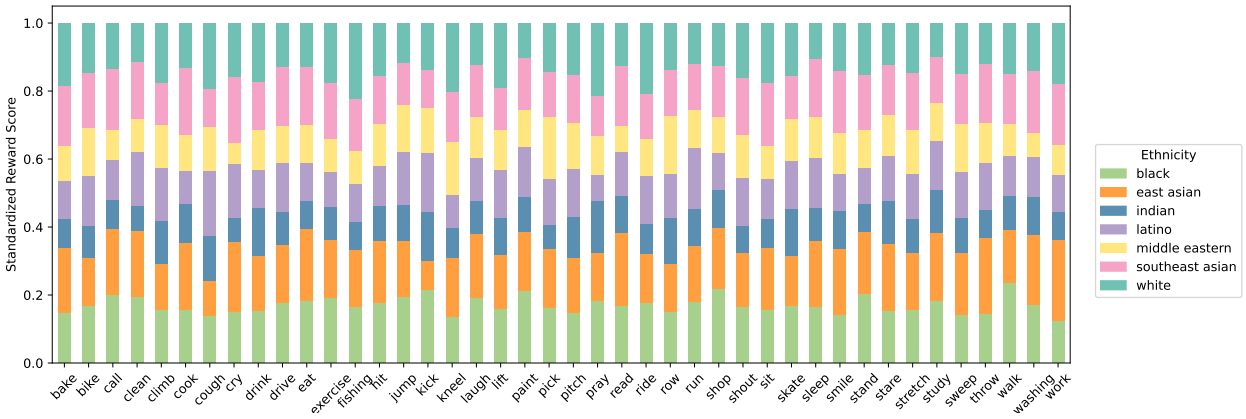

Figure 25: Ethnicity Bias - Pick Score

D Social Biases in Preference Alignment

Building on our analysis of gender and ethnicity biases in image reward models, we examine how preference alignment tuning affects bias in video generation. We fine-tune a Video Consistency Model distilled from VideoCrafter-V2 (VCM-VC2) Li et al. (2024) using three image-text reward models, HPSv2.0, HPSv2.1, and PickScore, and compare social bias distributions before and after tuning to assess how each reward model shapes identity representation. Following the T2V-Turbo-V1 training protocol Li et al. (2024), we incorporate reward feedback into the Latent Consistency Distillation process Luo et al. (2023) by using single step video generation. During student model distillation from a pretrained teacher text to video model, we directly optimize the decoded video frames to maximize reward scores from the image-text alignment models, guiding each frame toward representations more aligned with human preferences.

We evaluate aligned video diffusion models using our bias framework (§4). Table 5 reports two metrics: PBS_G for gender imbalance across ethnic groups, and RDS_e and SDI for ethnicity representation disparity and overall output diversity.

Ethnicity-Aware Gender Bias. We evaluate gender portrayals under the `ethnicity+person` condition using the previously defined PBS_G metric. A positive PBS_G score indicates a tendency to depict men more frequently, while a negative score suggests a preference for women. The base model, VCM-VC2, demonstrates a strong man bias across all ethnicities, which becomes more pronounced with alignment using HPSv2.0. In contrast, alignment with HPSv2.1 and PickScore significantly reduces PBS_G, indicating a shift toward more balanced or woman-preferred outputs. This change reflects the underlying woman bias present in the HPSv2.1 and PickScore reward models, which steer the model away from the man-dominant bias of the base model.Figures 26 to 33 presents the PBS_G scores across 42 actions for each ethnicity group.

Ethnicity Bias. Under the `ethnicity-only` condition, we analyze models' representation balance using the previously defined RDS_e and SDI metrics. Positive values indicate overrepresentation, and negative values indicate underrepresentation. Overall demographic balance is measured using SDI, where higher values reflect more equitable representation. The base model, VCM-VC2, strongly favors White individuals (RDS = 0.6405), while Black, East Asian, and Middle Eastern groups are underrepresented. Alignment with HPSv2.1 reduces some disparities by improving balance for White and Black groups, but significantly decreases Latino representation (RDS = –0.4352) and lowers SDI, indicating reduced diversity. In contrast, PickScore achieves the highest SDI and produces more balanced representation across most ethnic groups, resulting in the most demographically equitable outputs. Figure 34 shows the ethnicity bias across 42 actions.

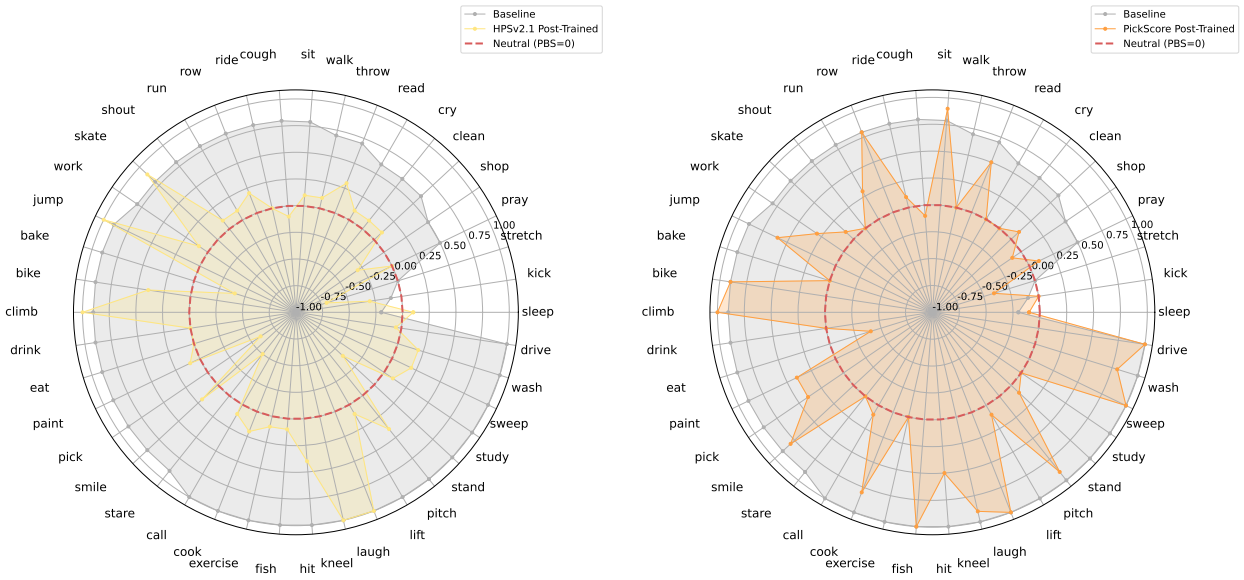

(a) HPSv2.1 vs. CLIP

(b) Pick Score vs. CLIP

Figure 26: Ethnicity-aware gender bias (White).

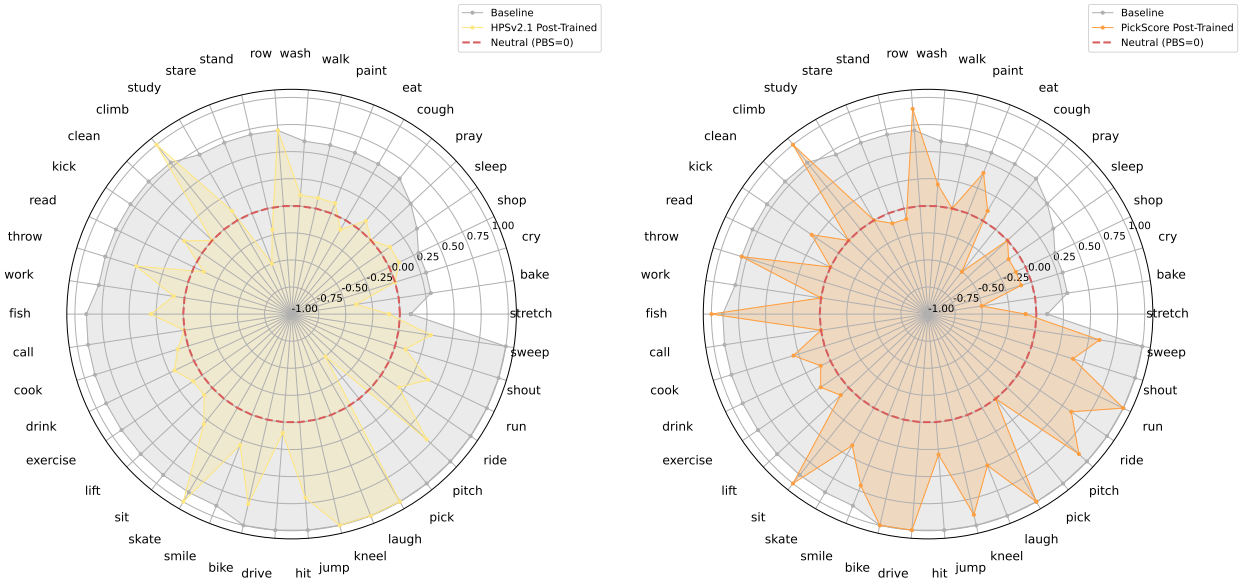

(a) HPSv2.1 vs. CLIP

(b) Pick Score vs. CLIP

Figure 27: Ethnicity-aware gender bias (Black).

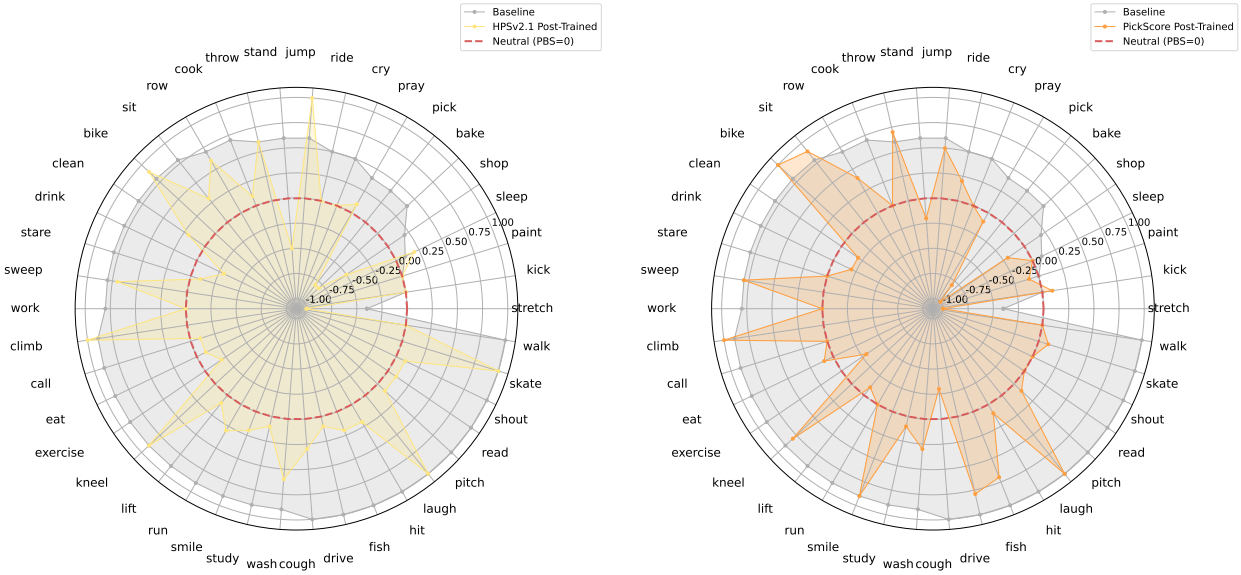

(a) HPSv2.1 vs. CLIP

(b) Pick Score vs. CLIP

Figure 28: Ethnicity-aware gender bias (East Asian).

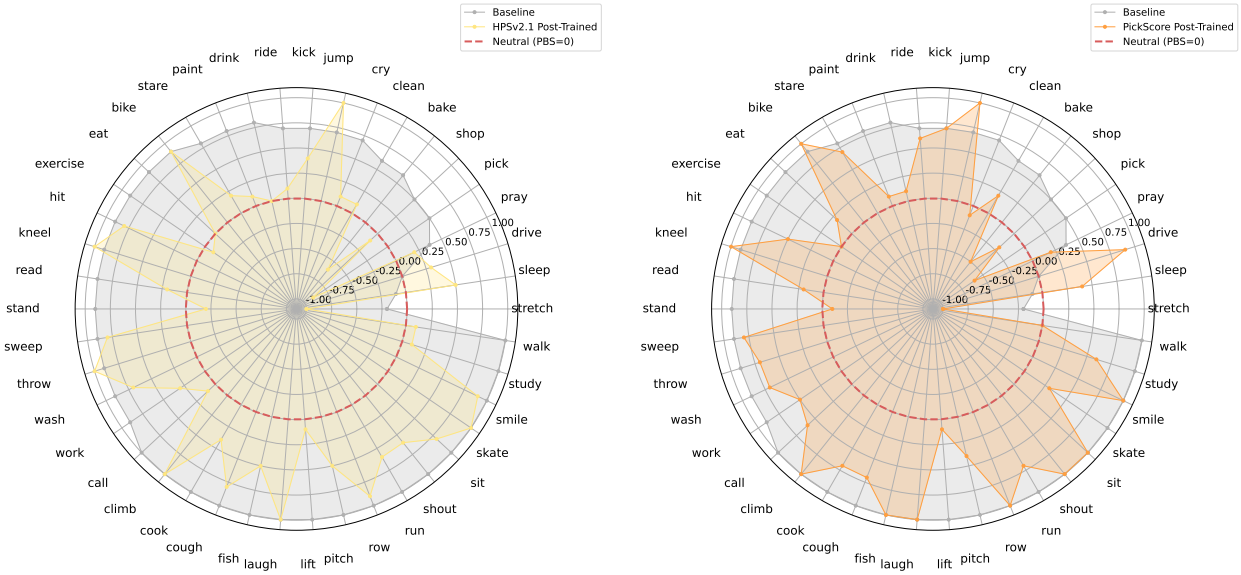

(a) HPSv2.1 vs. CLIP

(b) Pick Score vs. CLIP

Figure 29: Ethnicity-aware gender bias (Southeast Asian).

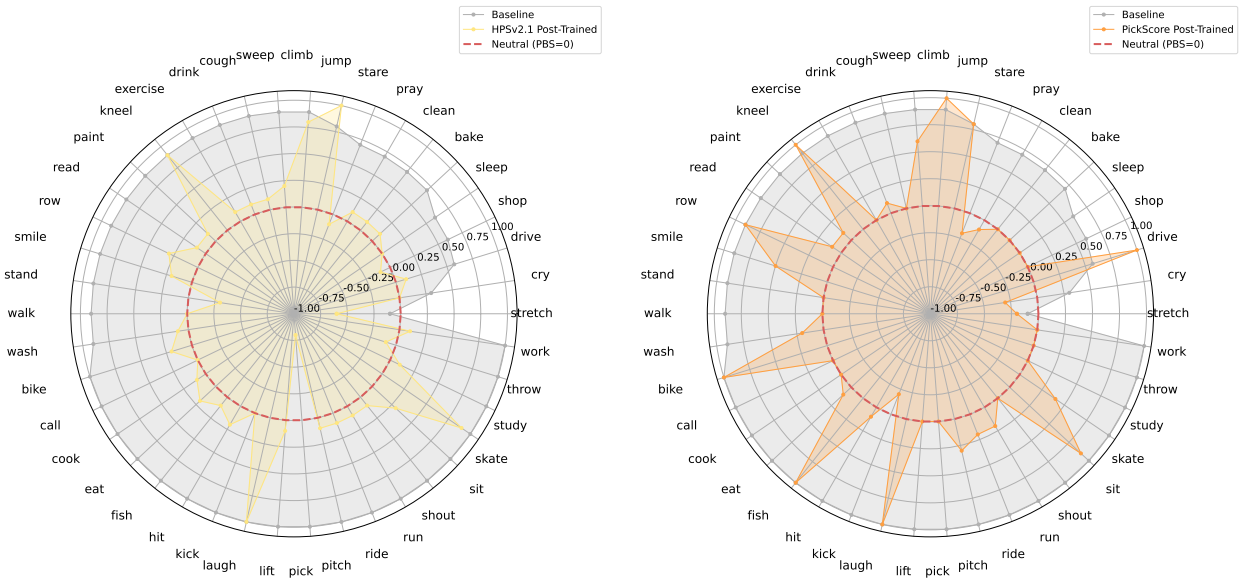

(a) HPSv2.1 vs. CLIP

(b) Pick Score vs. CLIP

Figure 30: Ethnicity-aware gender bias (Indian).

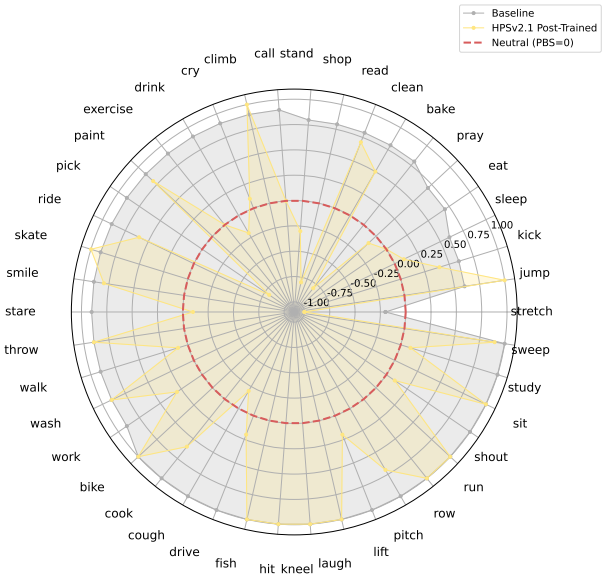

(a) HPSv2.1 vs. CLIP

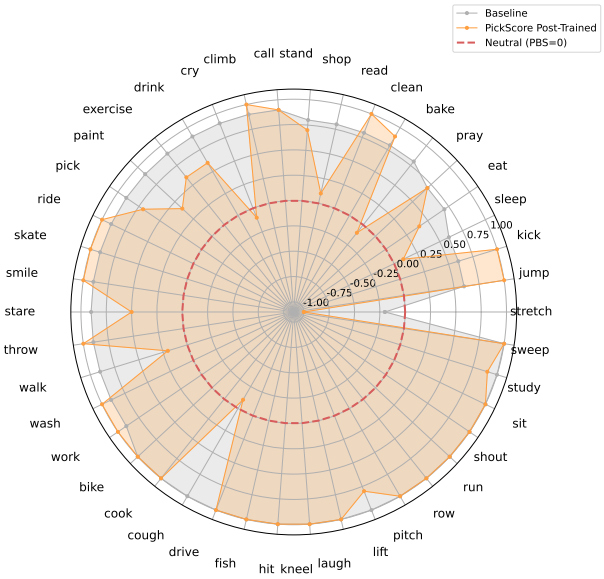

(b) Pick Score vs. CLIP

Figure 31: Ethnicity-aware gender bias (Latino).

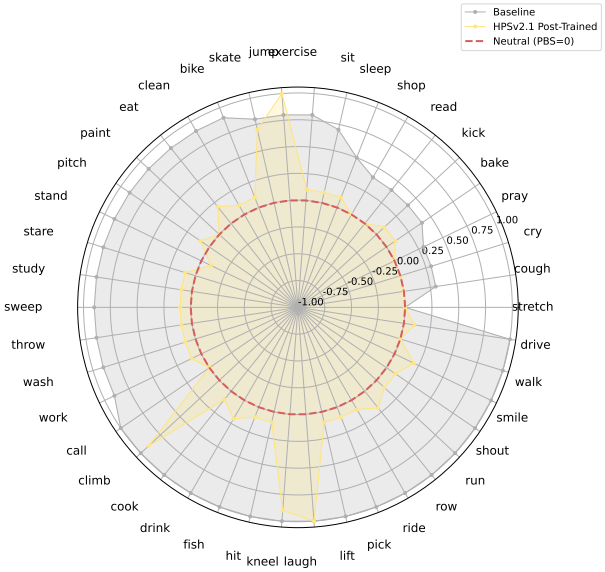

(a) HPSv2.1 vs. CLIP

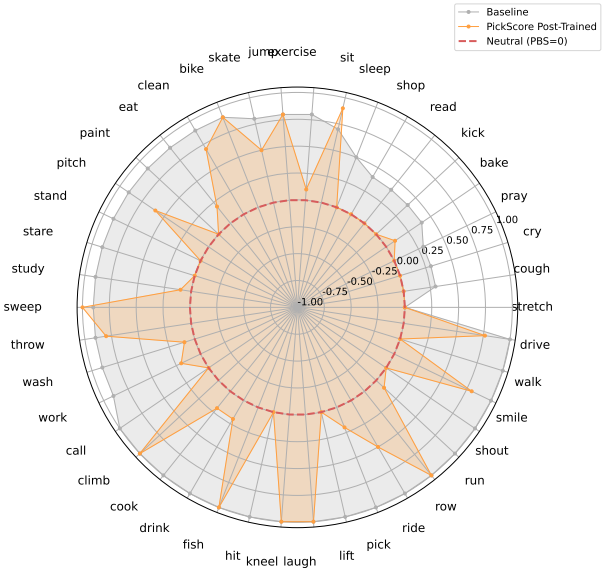

(b) Pick Score vs. CLIP

Figure 32: Ethnicity-aware gender bias (Middle Eastern).

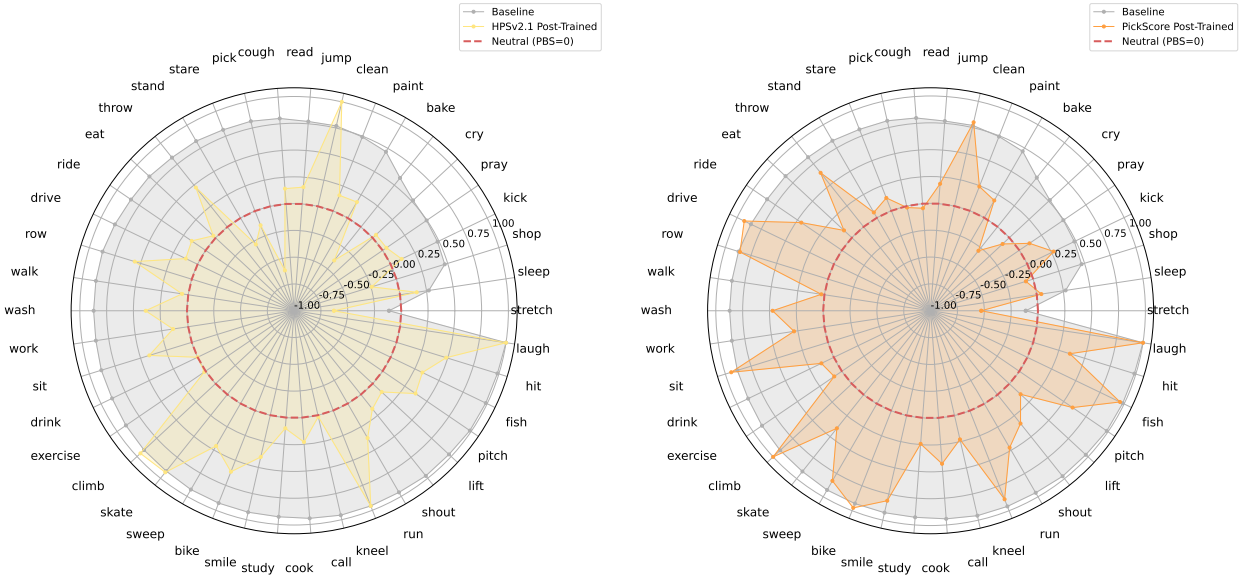

(a) HPSv2.1 vs. CLIP

(b) Pick Score vs. CLIP

Figure 33: Ethnicity-aware gender bias (averaged).

Figure 34: Ethnicity bias distribution

E Controllable Preference Modeling for Video Diffusion Models

Building on prior findings, we observe that reward models trained on imbalanced image preference datasets inherit and amplify social biases. These biases are then reflected in video diffusion models fine-tuned with such reward signals, often leading to unbalanced outputs. In this section, we explore whether manipulating the distribution of social attributes in image datasets allows for controllable bias in reward models, enabling video models to produce more equitable outputs Sheng et al. (2020).

E.1 Image Reward Dataset Construction

Building on the generated images from §5.1, we construct two case-specific reward datasets: one with a man-preferred bias and the other with a woman-preferred bias. The man-preferred dataset is designed to steer both the reward model and the downstream diffusion model toward favoring man representations. Conversely, the woman-preferred dataset encourages a shift toward woman representations. Notably, when applied to a base video diffusion model that exhibits a man-preference bias, the woman-preferred dataset can serve as an effective counterbalance, enabling the training of models with more equitable gender representation.

More specifically, we construct preference pairs using images from the `Gender+Ethnicity` dataset by selecting two images that depict the same action and belong to the same ethnicity group, one featuring a man and the other a woman (for example, images M-1 and W-1 in Figure 3). These image pairs are used to train reward models with prompts of the form: "A/An `[ethnicity]` person is `[action]`-ing `[context]`." For the man-preference dataset, we assign a reward score of 1 to the image with a man character and 0 to the image with a woman character. In contrast, f or the woman-preference dataset, we assign a reward score of 0 to the image with a man character and 1 to the image with a woman character. This process results in 2.94 million preference pairs in each dataset, calculated as 42 actions multiplied by seven ethnicity groups, with 100 male and 100 female images per group. To improve the representation of no-face content, we additionally incorporate 537,660 face-free image pairs from HPDv2, which enhances balance in our proposed reward datasets.

E.2 Image Reward Model Development & Alignment Tuning

Leveraging the man-preferred and woman-preferred image datasets introduced in §7.1, we fine-tune two reward models on top of a pre-trained CLIP vision encoder: the Man-Preferred Reward Model ($\mathrm{RM_M}$) and the Woman-Preferred Reward Model ($\mathrm{RM_W}$). Each model is trained to reflect gender-specific preferences based on its respective dataset. As shown in Table 7, $\mathrm{RM_M}$ consistently assigns greater PBS_G scores across all demographic groups, indicating a strong alignment with man-preferred representations. In contrast, $\mathrm{RM_W}$ exhibits an opposite trend, systematically favoring woman-preferred content. The clear divergence between these models highlights the effectiveness of reward tuning in capturing and reinforcing gendered preferences.

Building on our earlier reward model training, we applied $\mathrm{RM_M}$ and $\mathrm{RM_W}$ to guide alignment tuning of a base video diffusion model using the same preference-driven training strategy. These reward signals enabled the generation of two distinct variants: one aligned with man-preferred content and the other with woman-preferred content. As shown in Table 8, alignment with $\mathrm{RM_M}$ led to consistently greater PBS_G scores across all demographic groups, reinforcing man-preference bias. Conversely, alignment with $\mathrm{RM_W}$ resulted in substantially smaller scores, indicating a strong shift toward woman-preference bias. These results confirm that our controllable preference modeling approach can effectively modulate gender bias in video generation, offering a flexible mechanism to either amplify or reduce specific social tendencies in model outputs. Figures 35 to 39 presents the PBS_G scores across 42 actions for each ethnicity group.

E.3 Actions Correlation Analysis

We analyze the changes in the reward model preference for 42 events and the bias of the video generation model before and after post-training, using the training results from §7. In Figure 40, the horizontal axis represents the reward model preference (PBS_G), and the vertical axis represents the change in the video generation model's bias before and after post-training (Δ PBS_G). In Figure 41 and Figure 42, the horizontal axis represents the event, and the vertical axis represents the change in the video generation model's bias

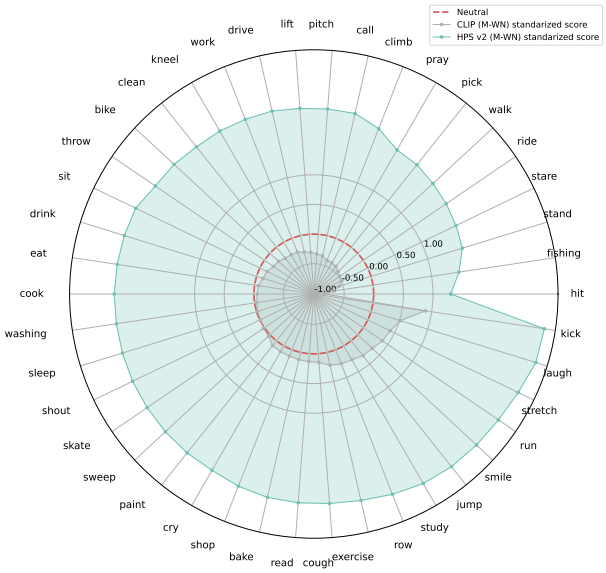

(a) Ethnicity-aware gender bias (averaged) of man-preferred reward model RM_M.

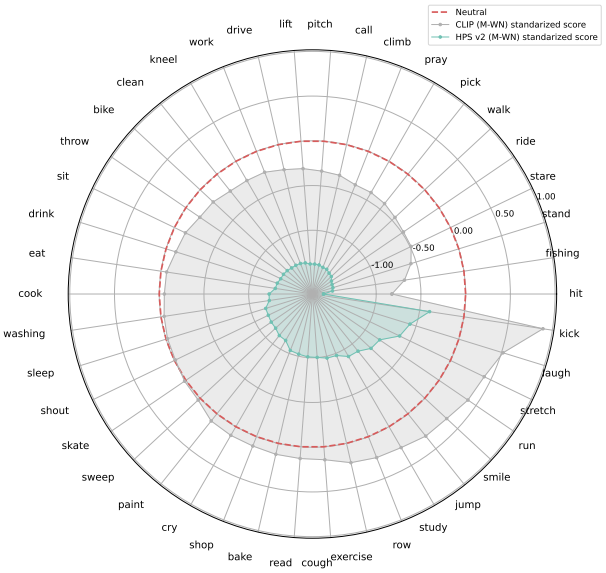

(b) Ethnicity-aware gender bias (averaged) of woman-preferred reward model RM_W.

Figure 35: Ethnicity-aware gender bias (averaged) of woman-preferred reward model RM_M and RM_W.

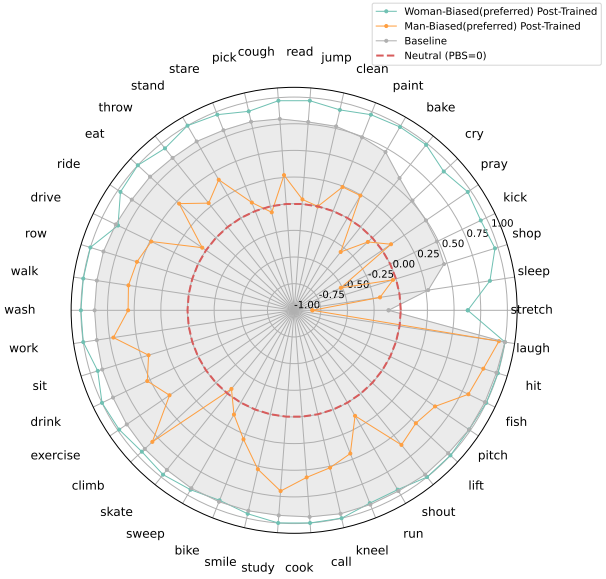

(a) Ethnicity-aware gender bias (averaged) of man-preferred and woman-preferred post-trained video generation model by reward model RM_M and RM_W.

(b) Ethnicity-aware gender bias (White) of man-preferred and woman-preferred post-trained video generation model by reward model RM_M and RM_W.

Figure 36: Ethnicity-aware gender bias (White) of man-preferred and woman-preferred post-trained video generation model by reward model RM_M and RM_W.

before and after post-training (Δ PBS_G) divided by the reward model preference (PBS_G). This ratio indicates the sensitivity of a particular event to the bias during post-training. We have arranged the events in the figure from left to right in ascending order of the vertical axis values; events further to the right are more sensitive.

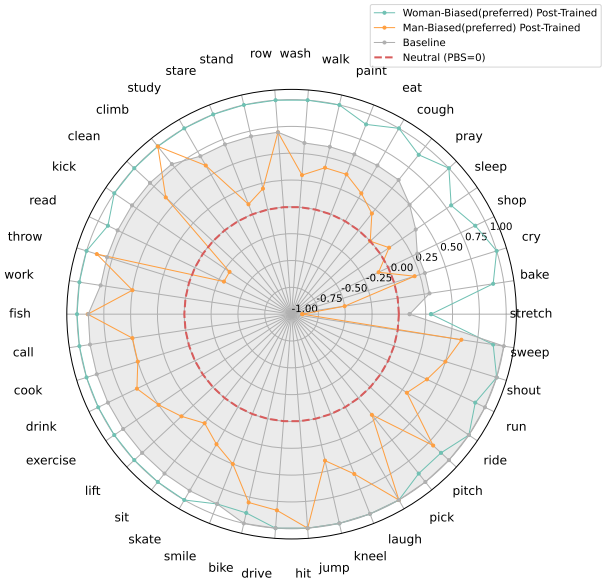

(a) Ethnicity-aware gender bias (Black) of man-preferred and woman-preferred post-trained video generation model by reward model RM_M and RM_W.

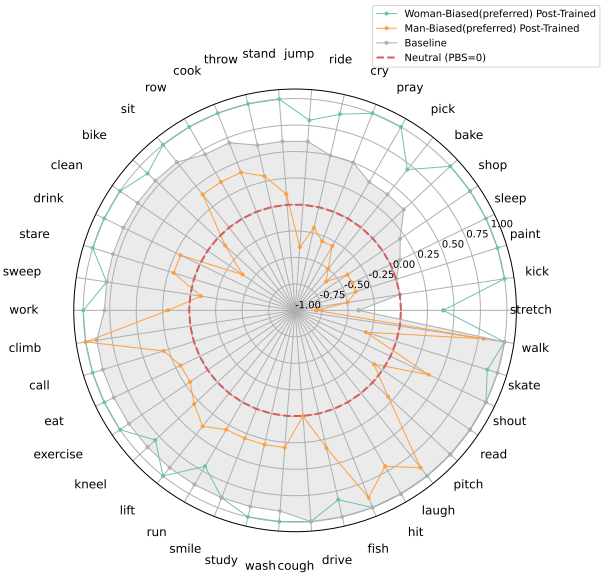

(b) Ethnicity-aware gender bias (East Asian) of man-preferred and woman-preferred post-trained video generation model by reward model RM_M and RM_W.

Figure 37: Ethnicity-aware gender bias of man-preferred and woman-preferred post-trained video generation model by reward model RM_M and RM_W.

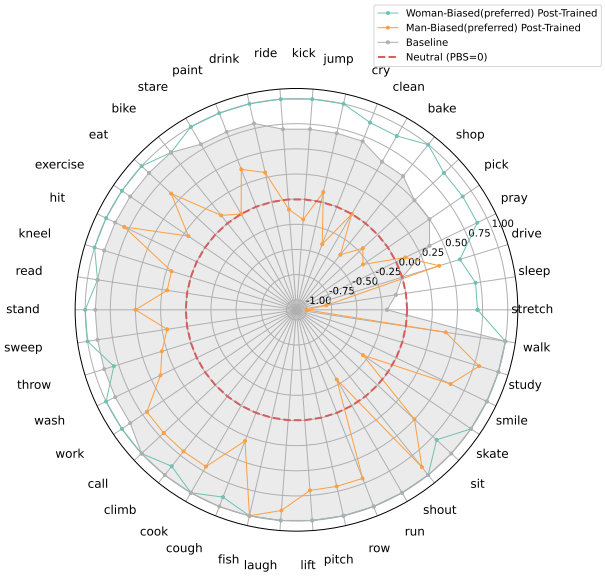

(a) Ethnicity-aware gender bias (Southeast Asian) of man-preferred and woman-preferred post-trained video generation model by reward model RM_M and RM_W.

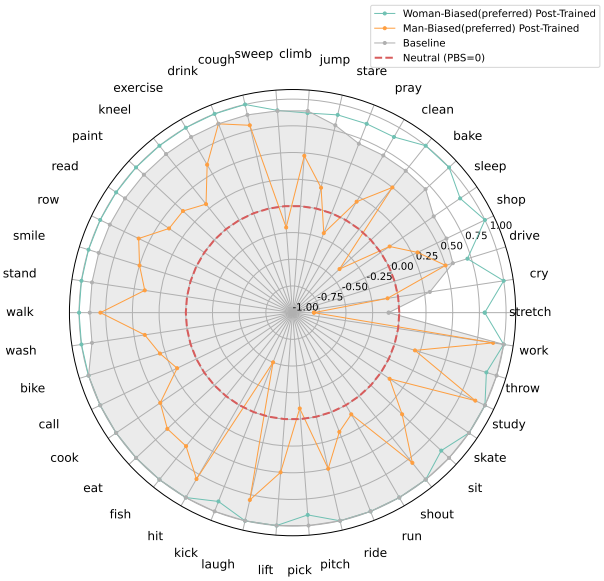

(b) Ethnicity-aware gender bias (Indian) of man-preferred and woman-preferred post-trained video generation model by reward model RM_M and RM_W.

Figure 38: Ethnicity-aware gender bias of man-preferred and woman-preferred post-trained video generation model by reward model RM_M and RM_W.

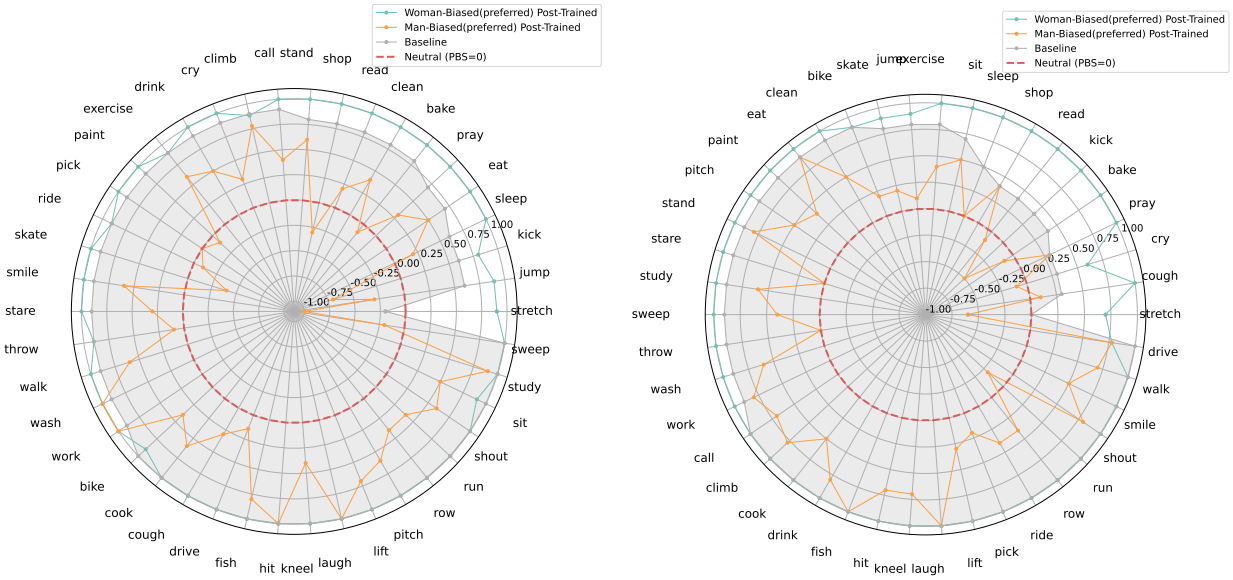

(a) Ethnicity-aware gender bias (Latino) of man-preferred and woman-preferred post-trained video generation model by reward model RM_M and RM_W.

(b) Ethnicity-aware gender bias (Middle Eastern) of man-preferred and woman-preferred post-trained video generation model by reward model RM_M and RM_W.

Figure 39: Ethnicity-aware gender bias of man-preferred and woman-preferred post-trained video generation model by reward model RM_M and RM_W.

F Reward Model Training and Inference Details

For both the training and inference of the reward model (RM), we largely followed the settings outlined in Wu et al. (2023). We also utilized the HPSv2 codebase available at `https://github.com/tgxs002/HPSv2` for these processes.

Training: We employed a batch size of 16 and the AdamW optimizer. The man-preferred and woman-preferred datasets that we constructed were adapted to the data loading format specified in the HPSv2 code (`https://github.com/tgxs002/HPSv2`). Ultimately, we trained the RMs for man-preferred and woman-preferred data for 1 epochs (equivalent to 23000 steps), with no data repetition within each step. The model training was initialized from a CLIP checkpoint.

Inference: We used the CLIP score as the inference score for the RM.

G Video Model Post-Training and Inference Details

For post-training during alignment tuning, we used the t2v-turbo-v1 codebase Li et al. (2024), available at `https://github.com/Ji4chenLi/t2v-turbo`. A reward model loss scale of 1 was applied. The video model was jointly trained with both the reward model loss and the diffusion loss over 200 steps, using data sampled from the WebVideo dataset.

For inference, we also utilized the same t2v-turbo-v1 codebase. Each inference setting was run 10 times with different random seed to ensure consistency and robustness of the results.

Figure 40: Δ PBS$_G$ of video generation model before and after alignment tuning by RM$_\mathrm{M}$ and RM$_\mathrm{W}$. Results are broken down into actions. Figure 41 and Figure 42 are based on this figure.

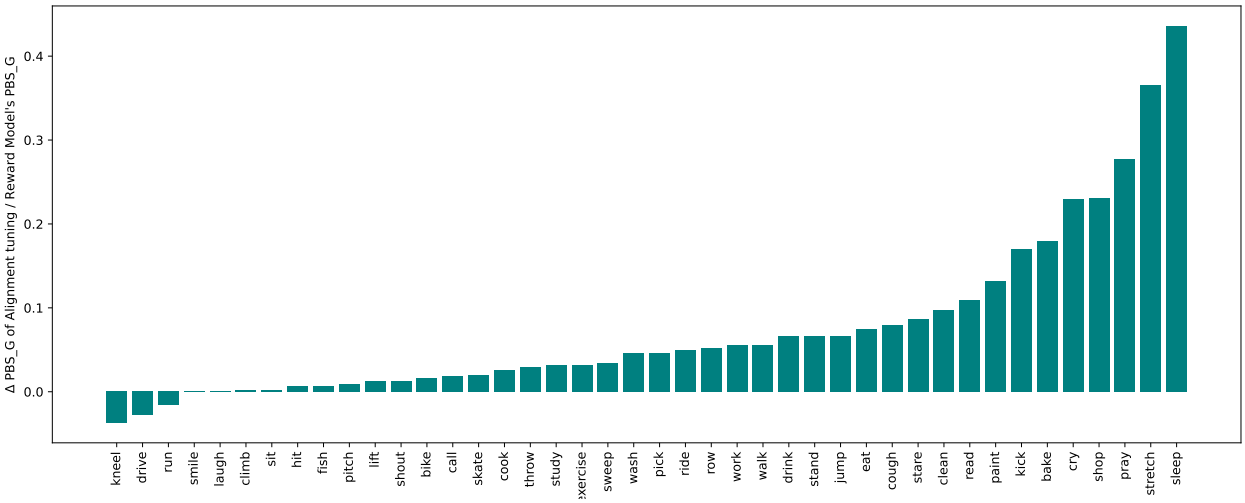

Figure 41: Sensitive actions in man-preferred post-training.

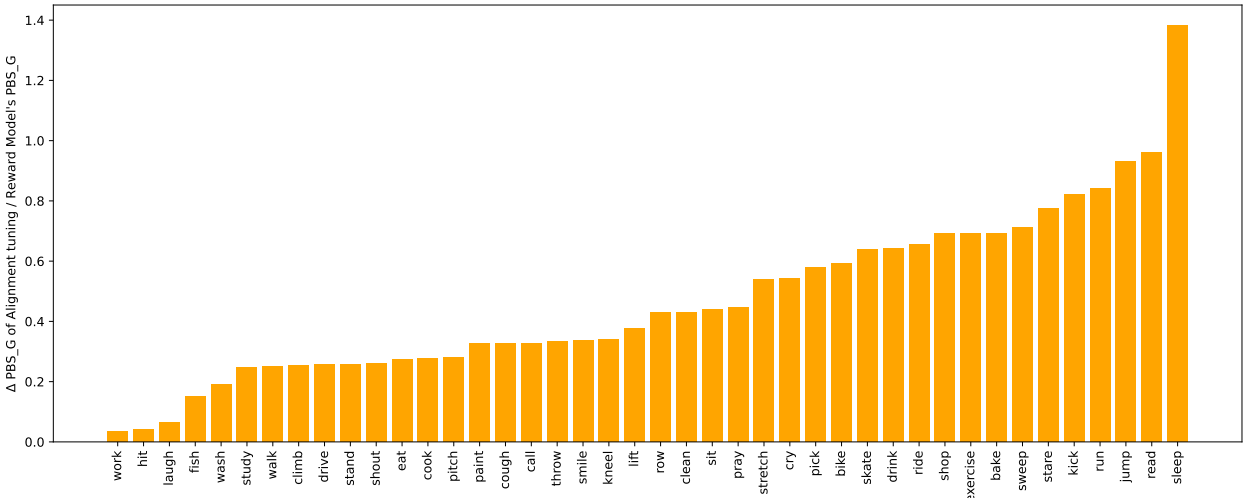

Figure 42: Sensitive actions in woman-preferred post-training.